

On the pressure equilibrium and timescales in the scale free convection theory

S. Pasetto^{a,e,b}, C. Chiosi^{c,*}, M. Cropper^e, E. Chiosi^d, D. Crnojević^{f,g}

^a*Dept. Integrated Mathematical Oncology (DIV Quantitative Science), H. Lee Moffitt Cancer Center and Research Institute SRB-4, 12902 USF Magnolia Dr. Tampa (FL), 33612, USA, email: Stefano.Pasetto@Moffitt.org*

^b*The Observatories of the Carnegie Institution for Science, 813 Santa Barbara St., Pasadena, CA 91101, USA*

^c*Department of Physics & Astronomy, "G. Galilei", University of Padua, Vicolo dell'Osservatorio 2, Padua, Italy, email: cesare.chiosi@unipd.it*

^d*INAF-Astronomical Observatory of Padua, Vicolo dell'Osservatorio 5, Padua, Italy, email: echiosi@libero.it*

^e*Mullard Space Science Laboratory, University College London, Holmbury St Mary, Dorking RH5 6NT, UK, email: m.cropper@ucl.ac.uk*

^f*University of Tampa, 401 West Kennedy Boulevard, Tampa, FL 33606, USA, email: Denija.Crnojevic@ttu.edu*

^g*Department of Physics & Astronomy, Texas Tech University, Box 41051, Lubbock, TX 79409-1051, USA*

arXiv:1909.13513v1 [astro-ph.SR] 30 Sep 2019

Abstract

Convection is one of the fundamental energy transport processes in physics and astrophysics, and its description is central to all stellar models. In the context of stellar astrophysics, the mixing length theory is the most successful approximation to handle the convection zones inside the stars because of its simplicity and rapidity. The price to pay is the mixing length parameter that is introduced to derive the velocity of convective elements, the temperature gradients in the convective regions and finally the energy flux carried by convection. The mixing length is a free parameter that needs to be calibrated on observational data. Pasetto et al. (2014) have proposed a new theory that determines all the properties of convective regions and the convective transport of energy with no need for a free parameter. In this study, we aim to discuss the merits of this new approach and the limits of its applicability in comparison with the mixing length theory. We present an analytical and numerical investigation of the main physical assumptions made by Pasetto et al. (2014) and compare them with the counterparts of the mixing length theory. We also present here the homogeneous isotropic limit of the Pasetto et al. (2014) theory and discuss some numerical examples to address and clarify misconceptions often associated with the new formalism.

Keywords: stellar structure; theory of convection; mixing-length theory

1. Introduction

Convection is one of the fundamental energy transport mechanisms in physics and astrophysics, and its description is central to all stellar models. Convection has been extensively studied over the years, and all attempts to model it have their origin in studies of turbulence, starting from the pioneering Kolmogorov work (e.g., Kolmogorov, 1941) up to the most recent computational simulations in physics (e.g., Ishihara et al., 2009; Lohse and Xia, 2010; Bec et al., 2010; Benzi et al., 2010; Rieutord and Rincon, 2010; Meneveau, 2011; Schmidt and Federrath, 2011; da Silva et al., 2014; Schumacher et al., 2014) and astrophysics (e.g., Rempel and Cheung, 2014; Hotta et al., 2015; Couch et al., 2015; Arnett et al., 2015; Gastine et al., 2015; Jiang et al., 2015; Kitiashvili et al., 2016; Lecoanet et al., 2016; Cristini et al., 2017). Excellent reviews can be found in Frisch (1998), Glatzmaier (2013) and Kupka and Muthsam (2017).

Stellar convection is customarily described by Mixing-Length Theory (MLT), a simplified analytical formulation of the energy transport by convection, developed long ago by Böhm-Vitense (1958). The MLT stands on previous studies by Biermann (1951) and Prandtl (1925). In the literature there are many

versions of the MLT, see e.g. Cox and Giuli (1968) and Kippenhahn and Weigert (1994), or their modern revisits, e.g. Weiss et al. (2004) and Kippenhahn et al. (2012), but all of them agree on the main lines.

The MLT stands on the basic (and largely justified by the common sense) assumption that the convective elements during their existence and motion are in rigorous hydrostatic equilibrium with the surrounding medium. This is used to derive an elementary equation of motion for the convective elements under buoyancy and gravity forces, to evaluate their kinetic energy and velocity, and then using the energy conservation principle to evaluate the total amount of energy stored by convective elements when they come into existence, the energy lost by radiative processes into the medium, and finally the net amount of energy released to medium when the elements dissolve in it (see Kippenhahn et al., 2012, Chap 6, Sec.6.1). The MLT makes use of the mixing length-scale to express the convective flux, velocity, and temperature gradients of the convective elements and stellar medium. The mixing length-scale is taken to be proportional to the local pressure scale-height, and the proportionality factor (the mixing-length parameter, MLP) must be determined by comparing the stellar models to some calibrator, usually the Sun. No strong arguments exist to suggest that the mixing-length parameter is the same in all stars and at all evolutionary phases. All the stellar models in literature are affected

*Corresponding author

by this basic drawback, i.e. the calibration of the MLP and the constancy of it with the stellar mass and evolutionary phases.

On one hand the assumption of rigorous hydrostatic equilibrium between convective elements and medium sounds reasonable at large scales because stars are in such a condition throughout their whole structure, including the convective zones in which the convective elements are supposed to originate, move and dissolve. On the other hand by using this condition to derive the physical properties of convection we miss the correct derivation of the motion and the energy transport by convection. The MLT copes with this drawback by introducing the mixing length, which is more than a free adjustable parameter, and in reality puts the incomplete physics on the right track. Indeed each convective cell (which is the fundamental vector of the convection) is born, lives and always dies outside any form of equilibrium, i.e., always outside hydrostatic-equilibrium too. In other words in astrophysics, the detailed treatment of pressure in the convective zones is often omitted or hidden beyond the assumptions of the MLT.

In a recent paper, Pasetto et al. (2014) (hereafter P14) presented an alternative theoretical framework that significantly differs from MLT in the fact that first it relaxes the local rigorous mechanical equilibrium between convective elements and medium, and second it does not require any freely tuned parameter (i.e., a mixing length) to determine the energy transfer inside the stars. We will refer to this theory as to the scale-free convection theory (SFCT).

In this paper, we study the cardinal differences between these two theories with particular attention to their pressure treatment. We want to emphasize and clarify the pressure adjustment as addressed by both the SFCT and the MLT. This will cast light on the physical meaning of the mixing length parameter itself and on some misunderstanding generated by the assumption of the delayed and immediate pressure adjustment assumed by SFCT and MLT respectively. In particular, we investigate the connection between the existence of a convective element, whose nature is by definition in a state of non-hydrostatic equilibrium, and the constant (time-independent) condition of hydrostatic equilibrium in which a star lives⁽¹⁾.

The plan of the paper is as follows. In Section 2 we cast light on the basic issue about the pressure field surrounding convective elements i.e. whether these latter are always in pressure equilibrium with surrounding medium. In Section 3 we elucidate the relevance of a correct temporal treatment of the pressure readjustment of the average convective element and its relation to the (always true) hydrostatic-equilibrium of the whole star, and with the aid of a simple semi-analytical case, we highlight the difference with respect to acceptance (not only) in the MLT that $Dp \equiv p_e - p^\infty = 0 \forall t \leq \infty$. In Section 4, with a simple numerical case, we check the SFCT and the limits of the so-called uniqueness theorem of P14. In section 5 we investigate numerical and theoretical limitations of the SFCT. In section 6, we highlight the relevance of the correct physical treatment of the dynamics in the convective layers of a star.

¹Thus, we are implicitly excluding stellar oscillations in this work for the sake of simplicity.

Finally in Appendix A we brief note on the non-inertial linear response theory for convective elements in spherical coordinates, of which the SFCT is a particular case.

2. The pressure field around convective elements

In common with MLT, the SFCT considers a star to consists of many layers. Each layer, say a layer L , is defined in the SFCT and MLT by its average pressure p , density ρ and temperature T respecting the classic hydrostatic equilibrium condition. The role of the SFCT, or the MLT, is to insert the amount of energy that has to be carried by the average convective element moving up and down the layers before the it starts to travel. If the pressure readjustment of any convective element is instantaneous, as in the MLT, there is apparently no transportation problem. If the pressure readjustment of the average convective element is not instantaneous but delayed by a physically meaningful finite speed velocity, as in a time-dependent SFCT, we need to check that the element does not start before the energy is inserted and ready to be sent.

The vectors carrying the energy are the eddies/convective elements. An eddy is a blob of vorticity with its associated velocity field \mathbf{v}_0 inside a bounded stellar medium L (²). In what follows, we will refer to any averaged convective element scheme as an eddy even though some of the adopted descriptions, e.g. the potential-flow approximation, do not consider vorticity in their formalism (they are curl-free). Any physical quantity in L cannot extend to infinity, because the layer is finite, therefore not representative of the whole star, and it does not last forever. In L the medium is described by the Navier-Stokes equations and it is characterized by an Equation of State (EoS) linking together the state variables such as the pressure $p = p(\mathbf{x}; t)$, density $\rho = \rho(\mathbf{x}; t)$, temperature $T = T(\mathbf{x}; t)$ at any position \mathbf{x} and time t .

The pressure field surrounding an eddy is obtained from the theory of potential (e.g., Kellogg, 1929; Jackson, 1975). This is before any assumption concerning the shapes of the eddies and the non-universal behavior of the convective turbulence. We start considering the fundamental proportionality relationship between pressure, density and the velocity field around a convective element (e.g., Batchelor and Proudman, 1956, Sec. 2)

$$p(\mathbf{x}; t) = \frac{\rho(\mathbf{x}; t)}{4\pi} \nabla_{\mathbf{x}}^2 \|\mathbf{x}\|^{-1} \int \mathbf{v}_0^T(\mathbf{x}'; t) \mathbf{v}_0(\mathbf{x}'; t) d\mathbf{x}' + \dots, \quad (1)$$

to the leading order, where $*^T$ is the transpose element and $\nabla^n [*]$ the power- n gradient operator applied to what is immediately on its right. This is the fundamental equation of convective turbulence (e.g., Batchelor and Proudman, 1956; Saffman, 1967).

We remark on aspects of Eq.(1):

²Mathematically, we can consider the layer to be mapped with a reference frame $S_0 : S_0(O, \mathbf{x}; t)$ with $L \subset \mathbb{R}^4$ assumed to be *compact* (i.e., bounded and limited) with O origin of the reference frame, spatial coordinates \mathbf{x} and temporal coordinate t . We can refer to S_0 as to an inertial reference frame to leave the notation S_1 for the non-inertial reference frames.

1. Eq.(1) is universally valid: it does not stand on the potential-flow approximation. It holds indeed for a fully rotational fluid too, where the concept of the eddy finds its natural definition.
2. Eq.(1) tells us how the pressure field associated with a convective element falls off and correlates with the motion of any other convective element across the generic layer, L , inside a star.
3. The right-hand side (RHS) of Eq.(1) is not constant, but retains an explicit dependence on time and position, meaning that the convective element is never required to be in equilibrium with its surrounding, and the pressure acting on it changes with time.
4. Hence, if a convective cell when born is not in pressure equilibrium with the surrounding medium, the same bubble dies inside a star long before reaching the condition of hydrostatic pressure equilibrium with the medium too ⁽³⁾. If we define $Dp \equiv p_e - p^\infty$, then clearly holds:

$$Dp \equiv p_e - p^\infty \neq 0 \forall t < \infty \quad (2)$$

where $p_e \equiv p(\mathbf{x}_e; t)$ is the pressure at a location \mathbf{x}_e on the eddy surface and $p^\infty \equiv \lim_{x \rightarrow \partial L} p(\mathbf{x}; t) < \infty$. This is always true if we assume L to be compact by Weierstrass's theorem⁽⁴⁾ is the pressure "far away" from the eddy surface (e.g., at the topological boundary ∂L).

Equation 1 forms the basis of turbulence theory and the transport of energy at different scales, times, and locations. This equation indeed shows how any small eddy can be considered as possible source (via the local pressure enhancement) of any other eddy in the environment under examination (i.e., L).

Probably the most straightforward eddy model in the literature is the one currently used in stellar astrophysics by the MLT (except for a few models of the Sun and other types of the star). Here an eddy is viewed as a (non-expanding) spherical body moving in an inertial reference frame $S_0(O, \mathbf{x}; t)$. While moving, the sphere instantaneously adjusts the pressure at its surface, i.e., the following condition is always satisfied:

$$Dp = p_e - p^\infty = 0 \quad \forall t.$$

The equation of motion for the barycenter, x_b , of the convective elements along its vertical motion is

$$\Delta x_b = \int_0^{t_L} \dot{x}_b dt = \Lambda_m h_p,$$

where Λ_m is the Mixing-Length that is usually supposed to be proportional to the pressure scale length h_p , and t_L is the lifetime of the convective element inside the layer L . This implies that while in the MLT the translational motion of the eddy is somehow taken into account, its expansion is ignored. In other words, if $\{\mathbf{x}_b, \mathbf{x}_e\}$ are the independent coordinates describing the

two degrees of freedom of an eddy (i.e., its position \mathbf{x}_b , and size $\|\mathbf{x}_b - \mathbf{x}_e\|$, for the translation and expansion/contraction description, with \mathbf{x}_e and element of the convective bubble surface), only one of them is taken into account. This is shown in Fig.1. The classical MLT is not entirely consistent with the temporal description of these two coordinates. We understand that encoded in the free parameter Λ_m there is not only the distance that a possible average element travels but much more:

1. the average energy exchanged between the mean flow and turbulence;
2. the differential behavior of intermittency (i.e., the irregular dissipation of kinetic energy) at different layers of the star;
3. the whole energy cascade as well as the temporal evolution required by the expansion in the second "omitted" independent coordinate;
4. and finally, that Λ_m quantifies the amount of energy carried by convection in a star to secure the observed luminosity and effective temperature.

In the astrophysical context, a coherent description of the temporal evolution of the pressure and motion of a convective eddy in relation to its independent coordinates is present in the SFCT proposed by P14. This approach stems from a more general theory of non-inertial gas linear-instabilities, where the Rayleigh-Taylor (RT) and Kelvin-Helmholtz (KH) instability treatment is included. As with the MLT, the SFCT assumes spherical symmetry for the convective eddy in order to simplify the mathematical formulation in the context of the potential-flow formalism. A description of the temporal and spatial pressure differences at the surface of a convective element with respect to the medium has been investigated and presented by Pasetto et al. (2016), hereafter P16, in the context of the SFCT. In that study (see their Fig.1) the temporal evolution of the pressure at the surface is compared with the hydrostatic equilibrium pressure of the stellar layer under consideration. The description of the convective elements presented by P14 and P16 takes the physics of non-hydrostatic equilibrium of the average eddy into account already in the definition of a convective element and includes the dependence of it on time (unlike the case of the MLT).

3. Capturing the essence of the SFCT

The correct description of the pressure and its variations essential for a correct formulation of the energy transport by convection/conduction/radiation, and the criteria for the onset of convection are indeed based on the comparison between the temperature over the pressure gradients $\nabla \equiv \lim_{x \rightarrow \partial L} \frac{\partial \ln T(\mathbf{x}; t)}{\partial \ln p(\mathbf{x}; t)}$, and $\nabla_e \equiv \lim_{x \rightarrow \mathbf{x}_e} \frac{\partial \ln T(\mathbf{x}; t)}{\partial \ln p(\mathbf{x}; t)}$, etc. for every t . Given the relevance of the pressure description inside a star, it is essential to highlight the implications of the pressure treatment adopted in the SFCT and to understand if the founding hypotheses of the SFCT can capture the real behavior of a convective blob rolling up in vortices of fluid.

³Sec.3.3, Appendix A, Pasetto et al. (2015).

⁴For our purposes, the Weierstrass theorems grants that a continuous function (e.g., the pressure p) on a compact set (e.g., L) is necessarily bounded.

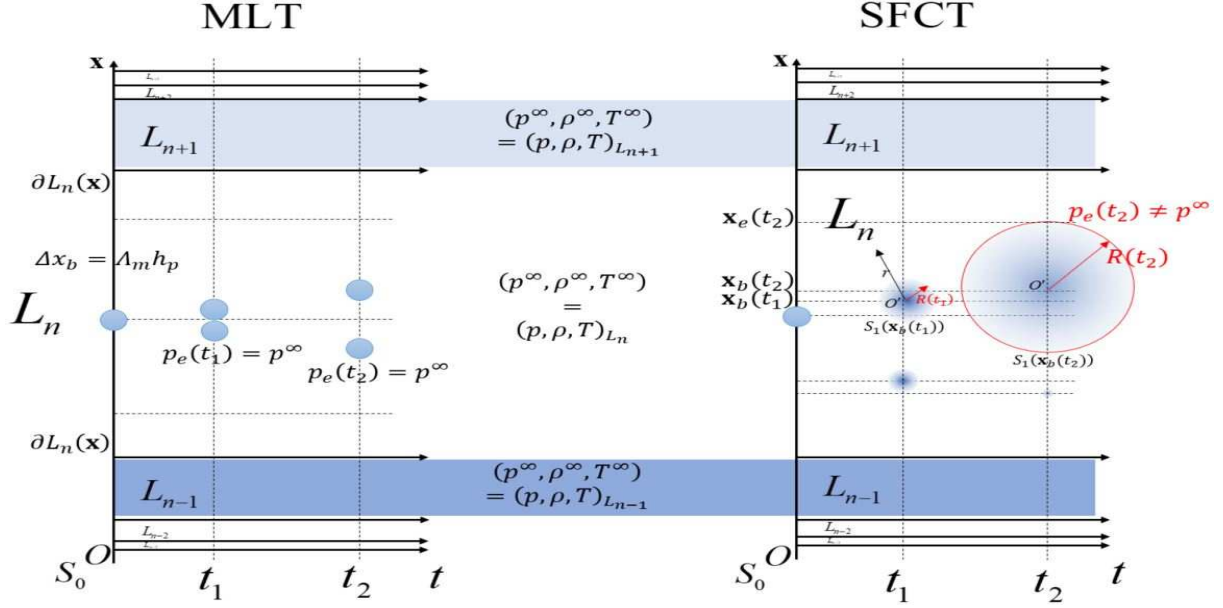


Figure 1: Pictorial representation of the temporal evolution of the same a convective element for MLT and SFCT. The star is discretized in M layers in hydrostatic equilibrium, L_n , with $n = 1, \dots, M$. The generic layer, L_n , is defined by the hydrostatic pressure, density, and temperature $(p, \rho, T)_{L_n}$. For both MLT and SFCT, these values are assumed to be time-independent and far away from the convective element, i.e., for every layer $(p^\infty, \rho^\infty, T^\infty) = (p, \rho, T)_{L_n} \forall t$. For the SFCT, each convective element is never in hydrostatic equilibrium with its medium; and the pressure, temperature and density at the convective element surface are $\{p_e(t), \rho_e(t), T_e(t)\} \neq \{p^\infty, \rho^\infty, T^\infty\}$. Upper and lower border of the layer are a function of the position, $\partial L_n = \partial L_n(x)$. The representation is purely indicative, the size of the layer L_n is typically much larger than the size of the convective element, say $\|L_n\| \gg R(t) \forall t$ for $n = 2, \dots, M - 1$.

3.1. SFCT homogeneous-isotropic limit case

A fundamental assumption on which SFCT stands is that the expansion/contraction rate of a convective element is much larger than the motion of its barycenter. In Fig.1 this is pictorially represented by the expansion of the convective element radius, R , being much larger than the vertical motion of the same element in the transition between two arbitrary instants t_1 and $t_2 > t_1$. If we follow the expansion/contraction in the non-inertial reference $S_1(O', \mathbf{r})$ co-moving with the barycenter of the convective eddy at velocity $v_{O'}$ (relative to the inertial system $S_0(O; t)$ whose origin is at the center of the star O), we can write this assumption as $\|\dot{\mathbf{r}}_e\| = \dot{R} \gg v_{O'}$. We physically motivate this approach because eddies are supposed to die shortly after their birth and to dissolve by RT and KH instabilities thus releasing their energy to the surrounding medium (see, e.g, Sec.3.3 and Appendix A). If the expanding/ shrinking elements of the SFCT capture the essential behavior of physical eddies rolling up in turbulent vortices, then we should be able to achieve reasonably good results in the pressure description even if we neglect their vertical motion entirely. This means to investigate the behavior of the SFCT as it approaches the limit case of a homogeneous-isotropic medium, a situation that can be easily achieved by nullifying the acceleration, i.e., setting $\mathbf{a}_{O'} = 0$, in the core equation of the SFCT⁽⁵⁾:

$$\frac{\partial \varphi_{v_1}}{\partial t} + \frac{1}{2} \langle \nabla_\xi \varphi_{v_1}, \nabla_\xi \varphi_{v_1} \rangle + \frac{p}{\rho} = f(t) - \langle \mathbf{a}_{O'}, \boldsymbol{\xi} \rangle, \quad (3)$$

⁵This is identical to Eq.(A.18) of Pasetto et al. (2015) and a direct consequence of our Eq.(1) from which it can be derived as shown in Pasetto et al. (2014).

with φ_{v_1} the velocity-potential flow for the stellar plasma in the non-inertial reference $S_1(O', \boldsymbol{\xi})$.

Without translation of the convective element the regime is that of homogeneous isotropic turbulence (e.g., Sagaut, 2008). In this simplification there is no net convective flow: this would be the case in which convective elements carry all the energy transport with little vertical motion but with significant expansion, the opposite of what is supposed to occur with the MLT in which only the vertical motion is considered. The scientific case we are investigating should be considered as a mathematical idealization meant to capture the essence of the role played by the sole expansion as compared to the case of the sole vertical motions.

We describe the expansion of a convective element with the formalism of the velocity-potential flow (e.g., Landau and Lifshitz, 1959). In the following, we will show that this simple description can capture the essence of the convective turbulence described by P14. In the absence of translation of the convective element, we can simplify our previous treatment in P14 from two reference frames moving relative to each other into a single static one. It is convenient to rationalize the notation as follows: $S_1(O', \boldsymbol{\xi}) \equiv S_0(O, \mathbf{x}) \forall t$ hence, by the assuming spherical coordinates in S_1 , we write $S_0(O, \mathbf{x}) \equiv S_0(O, \mathbf{r}) = S_0(O, r, \theta, \phi)$ where the system by spherical symmetry can be described merely by the evolution of the radius vector $\|\mathbf{r}\| \equiv r$ whose value at the convective element surface is the function of time $\|\mathbf{r}\|_e \hat{e}_r \equiv R(t)$.

Under these assumptions, the potential vector in S_0 is $\Phi_{v_0} = -\frac{\dot{R}R^2}{r}$ and the velocity field $\mathbf{v}_0 = \frac{\dot{R}R^2}{r^2} \hat{e}_r$. Given these premises, at an arbitrary but fixed time t the Bernoulli equation in S_0

becomes (see Eq.(3) and Fig.1):

$$\frac{\partial \Phi_{v_0}}{\partial t} + \frac{\|v_0\|^2}{2} + \frac{p}{\rho} = \text{cnst.}, \quad (4)$$

which with

$$\begin{cases} \frac{\partial \Phi_{v_0}}{\partial t} = -\frac{R(2\dot{R}^2 + R\ddot{R})}{r} \\ \frac{\|v_0\|^2}{2} = \frac{1}{2} \left\langle \frac{\partial \Phi_{v_0}}{\partial r}, \frac{\partial \Phi_{v_0}}{\partial r} \right\rangle = \frac{1}{2} \frac{R^4 \dot{R}^2}{r^4}, \end{cases} \quad (5)$$

becomes:

$$\frac{p(r;t)}{\rho(r;t)} + \frac{1}{2} \frac{R^4 \dot{R}^2}{r^4} - \frac{R(2\dot{R}^2 + R\ddot{R})}{r} = \text{cnst.} \quad (6)$$

We set the constant by requiring that far away from the sphere we have $p(\partial L;t) = p^\infty$ and $\rho(\partial L;t) = \rho^\infty$ for all t mainly because the size L of the layer is much larger than that of the eddy (see Fig.1). Note here that the formulation of the problem is entirely general, not requiring hydrostatic condition at the border of the domain of definition ∂L ; on the contrary $p(\partial L;t)$ could be taken to be any other pressure within L and outside the eddy without invalidating these arguments. This is implicit to the sharing of pressure information introduced by Eq.(1) whose applicability is entirely general. Nevertheless, we will assume that the stellar convective layer is always in rigorous hydrostatic equilibrium as a star is, i.e., SFCT correctly assumes hydrostatic-equilibrium at ∂L for each L and each t . Therefore, with these considerations and relaxing the time dependence only in ρ , we can complete the physical description in Eq.(6) with

$$\frac{p(r;t)}{\rho} + \frac{1}{2} \frac{R^4 \dot{R}^2}{r^4} - \frac{R(2\dot{R}^2 + R\ddot{R})}{r} = \frac{p^\infty}{\rho^\infty}, \quad (7)$$

which simplifies as:

$$\frac{\dot{R}^2 R^4}{2 r^4} - \frac{R}{r} (2\dot{R}^2 + R\ddot{R}) = \frac{p^\infty - p(r;t)}{\rho^\infty}. \quad (8)$$

This is either a differential equation for $R(t)$ if the pressure is given or an equation for the pressure field if $R(t)$ is given. We follow this second interpretation because from Eq.(B15) of P16 (see also Fig.A1 of P14) we have already learned that the interesting temporal evolution of the convective eddy is quadratic in time to the first order. This means that we can assume that the solutions of interest are those of type

$$\frac{R}{R_0} = 1 + \frac{t^2}{t_0^2}, \quad (9)$$

and we solve Eq.(7) as an equation for the pressure field. We look at a generic sphere instantaneously overlapping the expanding eddy with $R \propto t^2$, set $r = R(t)$ in Eq.(8), and make use of Eq.(9) to obtain:

$$\begin{aligned} \frac{\dot{R}^2 R^4}{2 r^4} - \frac{R}{r} (2\dot{R}^2 + R\ddot{R}) \Big|_{r=R} &= \frac{p^\infty - p(r;t)}{\rho} \Big|_{p=p_e} \Leftrightarrow, \\ \frac{1}{2} \frac{\tau^2 (1 + \tau)^8}{\chi^4} - \frac{(1 + \tau)^4}{\chi} \left(\frac{1}{2} + \frac{2\tau^2}{(1 + \tau)^2} \right) &= \frac{Dp}{p^\infty}, \end{aligned} \quad (10)$$

where for the sake of simplicity we set $\left\{ \frac{r}{R_0}, \frac{t}{t_0} \right\} \equiv \{\chi, \tau\}$ and we achieved standard non-dimensionality of the partial differential equation by setting $\frac{\rho^\infty}{\rho} \left(\frac{2R_0}{t_0} \right)^2 \equiv 1$. With a similar procedure the velocity field is:

$$\frac{v_r}{v_0} = \frac{2\tau(1 + \tau^2)^2}{\chi^2}. \quad (11)$$

with $v_0 \equiv \frac{R_0}{t_0}$. In this way, the expansion of the convective elements increases with time $\chi \propto \tau^2$ while it is immediately evident that to the leading order (i.e., by series expansion to ∂L) the pressure difference, Dp , drops with radius but increases with time as $Dp \propto \tau^2$ to follow the Bernoulli theorem. In particular the following temporal relation holds good:

$$\chi \propto \tau^2 \Rightarrow Dp \propto \tau^2, \quad (12)$$

which correlates the temporal evolution of the pressure at the convective element surface to that of the medium surrounding the convective element as imposed and predicted by Eq.(1). To better clarify the results we have obtained, we plot in Fig.2 and Fig. 3 the temporal and spatial dependence of the pressure and velocity fields around ideal convective elements as obtained in Eq.(10) and (11).

In Fig.2 the different lines represent the different temporal evolution of the pressure field. As time increases, the convective element grows in size as given by Eq.(9) and represented by the 3D spheres. It is soon evident that not only $Dp \neq 0 \forall t$, but even grows with time, contradicting the widespread notion that $Dp = 0$ (e.g., Eq.(6.2) in Kippenhahn et al., 2012). This is, as noted in Sec.1, indeed required from Eq.(1), the fundamental equation of convective turbulence. Only infinitely far from the convective element $Dp \rightarrow 0$, but this simplified scheme (and SFCT) fails because a stellar layer is not infinite nor it does last infinite time⁽⁶⁾. Since in this example, no hydrostatic equilibrium has been imposed, p^∞ can be the pressure existing at the surface of any nearby element. We also plotted for comparison in Fig.2 the spatial pressure dependence expected far away from the convective element in the case of rotational media (dashed line, Batchelor, 2000).

Similar considerations can be made for the velocity field surrounding a convective element as a function of time and position (see Fig.3). Note that the velocity of any fluid particle at the arbitrary location \mathbf{r} , $v_r = v_r(\mathbf{r}; t) \neq \dot{R}$ everywhere apart from the instantaneous location of the sphere overlapping the convective element surface as evident from Fig.3.

This case we have just illustrated is useful when compared to the more complex treatment presented in P14, and it helps to understand the meaning of the decoupled equations of the motion presented in Eq.(3) of P16 mentioned in the previous section. A few points are worth highlighting:

1. The pressure gradients presented in this simple case show the same asymptotic trends displayed in the more complex, non-inertial treatment of moving convective elements used

⁶It also fails mathematically because L has been assumed to be compact (finite in space and time).

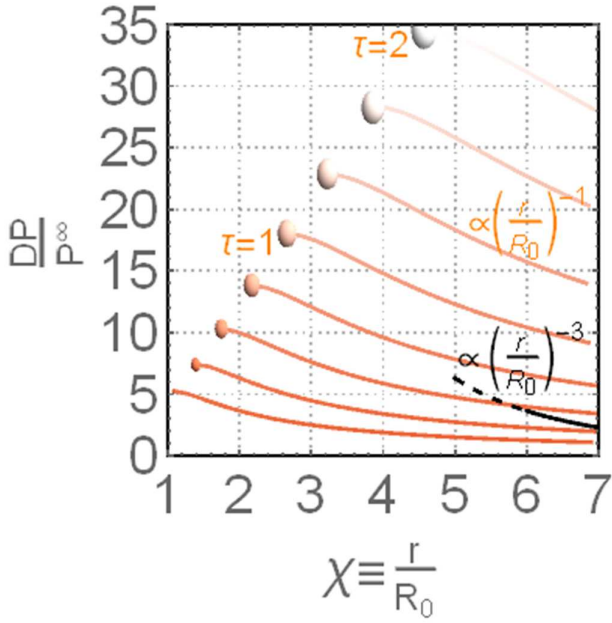


Figure 2: The temporal and spatial evolution of the relative pressure ratio between the value at the bubble surface and the one at infinity. Normalized time runs from $\tau = 0$ to $\tau = 2$ from the bottom to the top. The lines start at the current surface of the spherical element position that is marked with a sphere whose radius increases according to Eq.(9). The profiles starting from the surface of the different spheres show the variation of the relative pressure difference as moving far away from a sphere (surface of the generic convective element) throughout large distances. The lines refer to the case of fluid in the irrotational potential-flow approximation. The dashed line shows (limited to one case), the expected variation for a rotational flow. The disintegration of any generic convective element as time goes by is indicated here by drawing the spheres and lines with colors of lower and lower intensity.

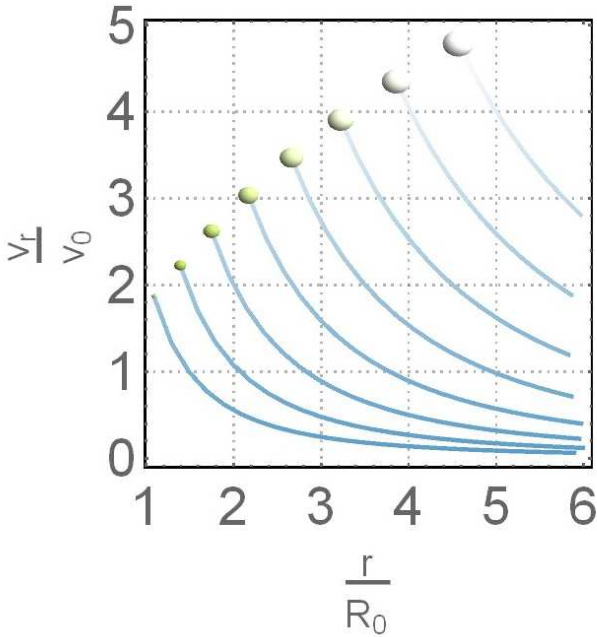


Figure 3: The same as in Fig.2 but for the velocity field surrounding the eddy.

by P14. At first glance, the ability of this simple exercise of capturing the essence of the SFCT may be somewhat surprising not only for the different formalism but also the different physical content. The SFCT *requires* both the hypotheses of hydrostatic-equilibrium far away from the convective element and the condition $\|\dot{\mathbf{R}}\| \gg v_O$, otherwise, the quadratic dependence of Eq.(12) is not formally met. Here neither is used, but the plot of Fig. 2 is very similar to that of Fig.1 in P16 where a similar trend was derived.

2. The velocity field shown in Fig. 3 tells us that the longer the elapsed time, the more the convective element expands/contracts, the less the approximation $Dp = 0$ holds true. The relationship between the radial dimension and time for the generic convective element, see Eq.(9) above, can be compared to which of Eq.(B15) of P16 that presents the same trend.
3. The velocity-potential formalism yields the trend of pressure across the medium and does not affect the vertical motion. The decoupling of the independent coordinates demonstrated by P16 (their Eq.3) using arguments based on Classical Mechanics about translation and expansion of convective elements is here clarified from hydrodynamic arguments based on the Bernoulli equation (Eq.(4)). This result strengthens the Corollary 1 in Section 4.2 of P14: the hydrodynamics of a single thin stellar layer can be considered subject to a constant acceleration throughout it (as far as Eq.(1) is concerned).
4. The temporal evolution of the pressure and expansion of the convective elements are intimately related and cannot be separated without violating the energy conservation principle (i.e., the Bernoulli theorem). If we want to examine the expansion/contraction of the convective elements, we cannot ignore the time evolution of the pressure and vice versa. This is done coherently in the SFCT but not in the MLT. The MLT copes with its fundamental failure in describing the temporal evolution of the system by introducing a free parameter that tacitly accounts for the conservation of the energy as a function of time.
5. The hypothesis $Dp = 0$ is *not* at the basis of the Schwarzschild and Ledoux criteria for instability, $\nabla_{\text{rad}} < \nabla_{\text{ad}} + \frac{\mathcal{L}}{\delta} \nabla_{\mu}$ as already proved in Lemma 2 of P14 and where ∇_{rad} , ∇_{ad} , ∇_{μ} are the classical radiative, adiabatic and molecular weight gradients as defined in Sec.3.

To summarize, what emerges from Figs.2 and 3 is that as the bubble expands, the pressure difference with the surrounding medium moves further away from equilibrium, rather than towards it. In this illustrating case where there is no translational movement of the bubble, the increase in size which is driving this evolution is put in by hand through Eq.(9), so that there is no need for concern at the source of energy to drive this process. In the complete treatment of P14 which encompasses the movement of the bubble, this expansion is self-consistently derived, and it is efficiently driven by the gradient of temperature and pressure gradients ∇ and ∇_e when a layer L becomes convective. We provide an illustrating check on this process in Sec.4. While the eddy expansion is taking place, instabilities set in,

destroying the bubble, as discussed in Sec.3.3 below.

3.2. The danger of the instantaneous pressure readjustment

Failing to understand Eq.(1), whose original analysis dates back to the milestone works of Batchelor and Proudman (1956); Saffman (1967), as well as failing the energy conservation required by the Bernoulli equation, can lead to incorrect results as in the recent work of Miller Bertolami et al. (2016, from now on MB16). While in the MLT the fundamental relation in Eq.(1) is implicitly hidden by a free parameter Λ_m , it is explicitly not fulfilled in the recent study of MB16. In light of the work reviewed in Sec.1 and the example in Sec.3.1, the analysis of the potential-vector approximation presented by MB16 is incorrect on three counts:

- the authors assume instantaneous hydrostatic equilibrium on the single bubble treatment. This is evident in the derivation of their Eq.(2) which does not contain any new free parameter as is provided by the MLT to compensate for the violation of the basic relationship of Eq.(1). In contrast, MB16 writes

$$\frac{dp(\mathbf{r};t)}{dt} = \frac{dp(\mathbf{r})}{dr} v_b(t)$$

so that for $v_b(t) = 0$, i.e. a bubble at rest, one has

$$\frac{dp(\mathbf{r};t)}{dt} = 0 \Leftrightarrow p(\mathbf{r};t) = p(\infty; t) = \text{cnst.}$$

However, this contradicts the fundamental equation of convection Eq.(1) that shows how the pressure at the surface of the bubble and infinity is never the same. The MB16 approach leads to their Eq.(8) that to our knowledge has no regime of validity. Later with their Eq.(A6) MB16 claim to prove that a convective element and medium have almost the same pressure. As well known since the early studies on the pressure fields around an eddy by Batchelor and Proudman (1956) and Saffman (1967) *this is never the case*. The works of Batchelor and Proudman (1956) and Saffman (1967) are well known and influential results that had a wide range of implications in physics and astrophysics (e.g., Rose, 1966; Lee and Tan, 1967; Forster et al., 1977; Moffatt, 1981; Bernard, 1983; Hunt and Carruthers, 1990; Kuznetsov et al., 1991; George, 1992; Hanazaki and Hunt, 1996; Skrbek and Stalp, 2000; Ossia and Lesieur, 2000; Moffatt, 2002; Poujade and Peybernes, 2010; Davidson, 2010; Meldi et al., 2011; Davidson et al., 2012; Teitelbaum and Mininni, 2012; Kitamura et al., 2014; Yakhot, 2014; Souldard et al., 2015; Rincon et al., 2017; Layek and Sunita, 2017; Zhou, 2017), over which SFCT stands, and that here we just proposed again in the example of Fig.2, where convective elements and medium have approximately the same pressure only for, say, $\tau \leq 1$ and never more as time passes⁽⁷⁾.

⁷Note that Fig.2 refers to the exercise of Sec.3. To obtain the correct numerical values for densities, temperatures, times, etc., the layer under examination has to be inserted into an environment given by an EoS of the star. This was already shown in Fig.1 of P16 and not repeated here.

- By construction, no equilibrium can exist for a convective element coming into existence. The authors assume instantaneous adjustment of the pressure equilibrium (see their Eq.(8)), i.e., MB16 do not take into account time/space evolution of pressure, but at the same time they follow the temporal evolution of the bubble size $\|\mathbf{x}_e(t)\|$ (one of the degrees of freedom of the system in S_O) and the motion $\mathbf{x}_O(t)$ (the other degree of freedom), which is mathematically and physically inconsistent.
- No turbulence can exist if the pressure adjusts itself instantaneously: the pressure waves caused by the pressure fluctuations at a given eddy position are indeed the trigger for the formation of other eddies and give rise to turbulent convection. While SFCT captures the fundamentals of this process, it is missing in MB16 (see, e.g., their result in Appendix Eq.(A6)).

The most obvious problem in MB16 is clear after our Eq.(12) (repeated here for simplicity):

$$\chi \propto \tau^2 \Rightarrow Dp \propto \tau^2,$$

at the surface of the convective element. Contrary to what shown here in compliance with the physics expressed by Eq.(1), MB16 derive their Eq. (A6) (which sustains their Eq.(2) and the rest of the paper) that predicts the opposite of our Eq.(12). The authors fail to investigate the limit of their Eq.(A6) because they compute the limit of $p = p(r, t)$ without examining whether the bubble exists in that regime in time and space. We have shown here that if Bernoulli's theorem is correctly fulfilled (and hence the energy conservation that it represents), it is never the case that $p^\infty \simeq p$ anywhere and at any time. Coherently, the velocity field is shown in Fig. 3 tells us that: the longer the elapsed time, the more the convective element expands/contracts, the less the approximation of Eq. (A6) in MB16 is verified. Indeed the correct physical formulation and analysis of the whole problem impose the pressure-time dependence of Eq.(12). In particular even far away from the bubble the condition $p^\infty \simeq p$ cannot happen because of the temporal divergence in the equations (in any case convective bubbles are destroyed by instabilities as examined in Pasetto et al. 2015 as time goes by)⁽⁸⁾.

3.3. The fate of a convective element

Finally, we examine the fate of an expanding/contracting convective element.

As already mentioned in P16 the SFCT fails in compressible regimes and in the very last layer of the star where suitable boundary conditions must be supplied⁽⁹⁾. Also, convective elements cease to exist at $t \rightarrow \infty$. The reason for this failure of the

⁸It can be proved by investigation of $\chi = 1 + \tau^n$ (with $n \in \mathbb{Z}$) that only for $n = 1$ the pressure at the surface $r = R(t)$ remains approximatively constant (it results in that $Dp \in [1.4, 0.0]$). This seems to be the only mathematical case in which the study of MB16 may be applicable or in which the immediate pressure balance between convective elements and the medium is established (see for instance Kippenhahn et al., 2012, their Eq. 6.2) even though, to our knowledge, no evidence exists where the proportionality $\chi = 1 + \tau$ is met.

⁹Note how in Fig.1 caption we exclude the layer L_n for $n = M$.

theory at significant times and very outer regions is that in our analysis we did not include the instabilities that dissipate and destroy the elements. Possible physical causes of disintegration include:

1. Deformation: the convective elements dissolve, losing their initial spherical geometry. This reflects the classical picture of a turbulent eddy that winds up in vortex sheets in a sequence of azimuthal vorticity and poloidal motions and sweeps angular momentum outward radially to form sheets. The start of this process is captured by the linear treatment regarding the stability parameter $\gamma_I^2 = \gamma_I^2(\mathbf{x}; t)$ already available in classical literature on the subject (e.g., Plesset, 1954).
2. Rayleigh-Taylor instability: finger-like penetrations of two fluids at different densities (e.g., a convective element expanding inside a radiative/convective fluid). The process depends on (i) the density difference between the two fluids; the instability parameter is $\gamma_{RT}^2 = \gamma_{RT}^2(\mathbf{x}; t)$, and (ii) the relative acceleration between the two fluids with instability parameter $\gamma_{a-RT}^2 = \gamma_{a-RT}^2(\mathbf{x}; t)$. See Appendix A for more details.
3. Kelvin-Helmholtz instability: the relative sliding of the inner layers concerning external ones of convective the elements helps to dissolve the convective element themselves. The instability parameter is $\gamma_{KH}^2 = \gamma_{KH}^2(\mathbf{x}; t)$. To the first order, no dependence on the acceleration of the convective element is found. See Pasetto et al. 2015 for an extensive investigation and Appendix A for more details⁽¹⁰⁾.

A convenient analytical solution is possible using the WKB approximation and a simple formulation for the linear-instability parameter results as:

$$\gamma^2 = \gamma_I^2 + \gamma_{RT}^2 + \gamma_{a-RT}^2 + \gamma_{KH}^2 + \gamma_{\text{mix}}^2, \quad (13)$$

see Eq.(A.5). Here γ_{mix}^2 refers to the linear superposition of the instability effects.

4. Numerical results of SFCT

After getting a better insight into the SFCT paradigm by studying how its behaves in the homogeneous isotropic case and in respect to the MLT, we pass now from the single eddy description to the collective averaged behavior of a system of convective cells embedded in a real stellar layer.

The generic layer L_n is always assumed to be in hydrostatic equilibrium both in the MLT and in the SFCT even though L_n is a sum of elements not in hydrostatic equilibrium (i.e., the convective elements). This description differs from the test-cases of Sec.3 because the single equation describing one eddy element is now embedded in a system of equations that describe

the layer L_n and the interaction of all the eddies with this layer. This single-to-collective description is achieved solely through a parameter (the mixing length Λ_m) in the MLT. The resulting set of equations is reported here (see, e.g., Eq.(B1) of P16):

$$\left\{ \begin{array}{l} \varphi_{\text{rad/cnd}} = \frac{4ac}{3} \frac{T^4}{\kappa h_p \rho} \nabla \\ \varphi_{\text{rad/cnd}} + \varphi_{\text{cnv}} = \frac{4ac}{3} \frac{T^4}{\kappa h_p \rho} \nabla_{\text{rad}} \\ v^2 = g\delta (\nabla - \nabla_e) \frac{l_m^2}{8h_p} \\ \varphi_{\text{cnv}} = \rho c_p T \sqrt{g\delta} \frac{l_m^2}{4\sqrt{2}} h_p^{-3/2} (\nabla - \nabla_e)^{3/2} \\ \frac{\nabla_e - \nabla_{\text{ad}}}{\nabla - \nabla_e} = \frac{6acT^3}{\kappa \rho^2 c_p l_m v}, \end{array} \right. \quad (14)$$

The same connection single-to-global description can also be achieved in the SFCT with this set of equations (see, e.g., Eq.(B21) of P16):

$$\left\{ \begin{array}{l} \varphi_{\text{rad/cnd}} = \frac{4ac}{3} \frac{T^4}{\kappa h_p \rho} \nabla \\ \varphi_{\text{rad/cnd}} + \varphi_{\text{cnv}} = \frac{4ac}{3} \frac{T^4}{\kappa h_p \rho} \nabla_{\text{rad}} \\ \frac{\bar{v}^2}{R} = 4g_4 \frac{\nabla - \nabla_e - \frac{\varphi}{\delta} \nabla_\mu}{\frac{3h_p}{2\delta\bar{v}\tau} + \nabla_e + 2\nabla - \frac{\varphi}{2\delta} \nabla_\mu} \\ \varphi_{\text{cnv}} = \frac{1}{2} \rho c_p T (\nabla - \nabla_e) \frac{\bar{v}^2 \tau}{h_p} \\ \frac{\nabla_e - \nabla_{\text{ad}}}{\nabla - \nabla_e} = \frac{4acT^3}{\kappa \rho^2 c_p} \frac{\tau}{R^2} \\ R = g_4 \bar{\chi} \frac{\nabla - \nabla_e - \frac{\varphi}{\delta} \nabla_\mu}{\frac{3h_p}{2\delta\bar{v}\tau} + \nabla_e + 2\nabla - \frac{\varphi}{2\delta} \nabla_\mu}. \end{array} \right. \quad (15)$$

Here all the quantities are averaged on their values at the generic layer $L_n(\mathbf{x})$ of Fig.1. In particular, for the sake of notation, we simplify the notation for $T(L) = T(\mathbf{x}) = T^\infty$ in T for the temperature, p^∞ in p for the pressure, and so forth, for density ρ , opacity κ , specific heat at constant pressure c_p , pressure scale length h_p , the gravity $g_4 = g/4$, radiative/conductive flux $\varphi_{\text{rad/cnd}}$, convective flux φ_{cnv} , adiabatic gradient ∇_{ad} , radiative gradient ∇_{rad} ; and where we adopt the standard notation $\delta \equiv -\frac{\partial \ln \rho}{\partial \ln T} \Big|_{p,\mu}$, $\varphi \equiv \frac{\partial \ln \rho}{\partial \ln \mu} \Big|_{p,T}$ with μ molecular weight. Here, a is the radiation pressure constant and c the speed of light.

Note how the mathematical nature of these two systems is profoundly different. In the MLT case, the system of Eq.(14) is local and time independent (i.e. pertinent the layer L_n at every time): it can be solved at every location \mathbf{x} where the defining quantities of L result well defined. The case of the SFCT system of equation is intrinsically more complex because of its time dependence. In Eq.(15) enter both time and location dependent quantities, i.e. the equations of motion for the average eddy, together with time-independent but location-dependent

¹⁰Note that the theory is presented in P16 for the specific case of a cloud at much higher temperature moving through an ionized plasma. However, the theory applies to any non-degenerate, non-relativistic gas in a convective zone inside a star.

quantities, i.e. the equations related to the Schwarzschild or Ledoux criteria and to the radiation transfer processes⁽¹¹⁾.

4.1. A simple numerical validation of the SFCT

We present here a simple numerical test of whether the SFCT can eliminate the mixing-length and why the uniqueness theorem presented in P14 holds good. As a result of this test, not only may we better understand the theory of P14 but also a numerical counterpart will be available to the analytical derivation of the set of equations presented by P16. The test does not require complicated stellar structure codes; instead, it can be followed with a pocket calculator.

We choose the same layer of the standard solar model already examined by P14. The layer is close to the surface where energy transport is far from being super-adiabatic, hence where the effect of the SFCT (or MLT) is more substantial and relevant. We use the same input values for our calculation in both MLT and SFCT and adopt SI units. The input values are, $r = 6.92002 \times 10^8$ m, $T = 48503.4$ K, $\nabla_{\text{ad}} = 0.28310$, $\nabla_{\text{rad}} = 0.295186$, $p^\infty = 2.05058$ N m⁻², $g = 277.517$ m s⁻², $\rho = 0.345519$ kg m⁻³, $c_p^\infty = 102986.2$ J kg⁻¹ K for stellar radius, temperature, adiabatic gradient, radiative gradient, pressure of the stellar layer far away from the convective element, gravity in the same layer, average density and specific heat at constant pressure far away from the convective element respectively. In addition to these values, three universal constants must be specified: gravity constant $G = 6.67428 \times 10^{-11}$ m³ Kg⁻¹ s⁻², the gas radiation density constant $a = 7.56464 \times 10^{-16}$ J K⁻⁴ m⁻³ and the speed of light $c = 2.99792 \times 10^8$ m s⁻¹.

We first obtain a solution for the radiative-convective-conductive transport of energy with the MLT. For this we use Eqs.(B1), (B2) and (B3) of P16. To proceed we need the mixing-length of $l_m = \Lambda_m h_p$ with $\Lambda_m = 1.64$ and $h_p = \frac{p}{\rho g}$ (e.g., Bertelli et al., 2008). With these entries, we can define the quantities V and W of Eq.(P16,B2), that we report here for simplicity and we evaluate as:

$$V = \frac{3acT^3}{c_p \rho^2 \kappa l_m^2} \sqrt{\frac{8h_p}{g\delta}} = 1.95043 \times 10^{-11}$$

and

$$W = \nabla_{\text{rad}} - \nabla_{\text{ad}} = 295186.3.$$

The expression for Eq.(P16,B3) becomes

$$\begin{aligned} & (x - 1.950 \times 10^{-11})^3 + \\ & + (1.733 \times 10^{-11})(x^3 - 2.951 \times 10^5) = 0 \end{aligned}$$

¹¹This sets the SFCT in that branch of Mathematics called Differential Algebra (e.g., Goode and Annin, 2015, see also P14) and its defining system is indeed an algebraic-differential system (DAS) of equations. The reduction of the original DAS to the system of Eq.(15) is achieved in P14. In the case of the Eq.(15) a theorem (Theorem of uniqueness, P14) grants that the solution of the system in terms of the mean stream velocity \bar{v} , convective flux φ_{cnv} , radiative/conductive flux $\varphi_{\text{rad/cnd}}$, stellar gradient ∇ , and eddy gradient ∇_e , exists and it is unique once the layer $L = L(T, \kappa, \rho, \nabla_{\text{rad}}, \nabla_{\text{ad}}, \nabla_e, g, c_p)$ is assigned (with $\bar{\chi}$ monotonic function of the parameter τ). The simple algebraic system of equation for the MLT is studied elsewhere (e.g., Kippenhahn and Weigert, 1994).

with

$$x^2 = \nabla - \nabla_{\text{ad}} + V^2.$$

This is the classic cubic equation of the MLT. Using now Eq.(B4), (B5) and (B6) of P16 one can derive the analytical solution. Alternatively, a numerical solution can be used (e.g., Press et al., 1992) to obtain $x = 0.01723$ for our layer. Finally, with this value for x we derive the layer pressure gradient as $\nabla = 0.28340$.

We repeat now the same calculations but using the SFCT for which no assumption has to be made for the mixing length parameter Λ_m simply because this parameter is missing in the equations of this theory. We start from Eq.(12) of P16, and we proceed backward to obtain ∇ . We use the same input values and take time interval sufficiently long, say $t > t^{(\infty)}$, to ensure that the asymptotic regime is reached for all relevant quantities (the velocity in particular)⁽¹²⁾. From a numerical point of view, we consider the asymptotic regime to be reached when the velocity of convective elements no longer change more than a few percent (the corresponding integration time is about $t < \infty \equiv t^{(\infty)} = 10^6$ s). The basic quintic equation of the system Eq.(15) is given by⁽¹³⁾

$$\sum_{i=0}^5 c_i \bar{v}^i = 0, \quad (16)$$

whose coefficients are, and take the numerical values:

$$\begin{aligned} c_5 &= 1, \\ c_4 &= \frac{h_p}{2\delta \nabla_{\text{ad}} \tau} = 37.7687, \\ c_3 &= \frac{8\alpha(\nabla_{\text{ad}} + 2\nabla_{\text{rad}})}{9\nabla_{\text{ad}} \tau} = 3.75137, \\ c_2 &= \frac{4\alpha(2\delta g_4 \tau (\nabla_{\text{ad}} - \nabla_{\text{rad}}) \sqrt{\bar{\chi}} + 3h_p)}{9\delta \nabla_{\text{ad}} \tau^2} = 3.75 \times 10^6, \\ c_1 &= \frac{32\alpha^2 \nabla_{\text{rad}}}{3\nabla_{\text{ad}} \bar{\chi}} = 0.000546, \\ c_0 &= \frac{16\alpha^2 h_p}{3\delta \nabla_{\text{ad}} \tau \bar{\chi}} = 1.97995 \times 10^{-8}, \end{aligned} \quad (17)$$

with

$$\alpha \equiv \frac{acT^3}{\kappa \rho^2 c_p}. \quad (18)$$

¹²It is worth recalling here that the asymptotic regime is a consequence of the uniqueness theorem (see P14, Sec.6.2). By itself, the single eddy equation of motion does not predict any asymptotic value. In particular, the SFCT does not apply at all in the case of a bubble rising in a medium and reaching the terminal velocity of traditional mechanic systems. As shown in Sec.3.3, the convective cell dissipate far before reaching any terminal velocity by instability effects. The asymptotic regime evidence in P14 and P16 (and hereafter referred to with $t > t^{(\infty)}$) manifests itself only when we embed the averaged single equation of motion for the convective eddy inside the system of equation of the convective layer. The solution of those six equations in Eq.(15) (i.e., once simultaneously considered) presents an asymptotic behavior; by itself the single equation of motion of SFCT does not.

¹³A note on the notation: here all the quantities of the SFCT (as well as for the MLT) refer to the average behavior over the layer L . Nevertheless, only for the velocities \bar{v} and the expansion function $\bar{\chi}$ we use an upper bar to distinguish them from the single bubble value in order not to confuse them with the previous section notation. The process of average for \bar{v} and $\bar{\chi}$ is detailed in P14 and in the next section too.

This equation has three real solutions and two complex ones. The only physically acceptable solution is $\bar{v} = 194.607 \text{ m s}^{-1}$. After the selection of the roots, the determination of ∇ becomes straightforward. Finally, we obtain $\nabla_{\text{SFCT}} = 0.28310$ for the stellar layer under examination which is virtually indistinguishable from the result above of the MLT: $\nabla_{\text{MLT}} = 0.28340$. The ‘‘mixing-length problem’’ is numerically solved: equalities between the left-hand side (LHS) and right-hand side (RHS) of the system of equations are recovered and verified (within the precision error) and the Sun modelled with MLT and with SFCT is the same, i.e., it has the same star pressure-temperature stratification.

4.2. Time dependence Schwarzschild or Ledoux criteria

By extending the detailed study of the stellar model to different phases of a solar track as in P16, we obtain the Figs. 4, 5, and 6 from which to extract a few essential features of the SFCT treatment.

While, generally, the stability criteria of Schwarzschild or Ledoux express the condition for the onset of the convection, they do not predict the timescale for a layer becoming convective. This is because they are not time-dependent criteria. The SFCT being a time-dependent theory, theory predicts a non-zero time-lapse for the convection to become effective. For the sake of simplicity, we refer to a stellar layer L as ‘‘convective,’’ if (and only if) both the conditions

$$\begin{cases} \nabla_{\text{rad}} > \nabla > \nabla_e > \nabla_{\text{ad}} \\ \varphi_{\text{rad/cnd}} < \varphi_{\text{cnd}} \end{cases} \quad (19)$$

are satisfied $\forall t$. Despite all the figures refer to layers where classic Schwarzschild criterion is satisfied, $\nabla_{\text{rad}} > \nabla > \nabla_e > \nabla_{\text{ad}}$, the onset of the convection is initially still radiative dominated energy transfer, i.e., $\varphi_{\text{rad/cnd}} > \varphi_{\text{cnd}}$, and only after a small time of the order of 100 seconds for a solar-like star (but which can be as large as 10^7 s for a giant star) the energy flux becomes dominated by convection (i.e., both the criteria of Eq.(19) are matched). Finally, we note how the timescale with which $\nabla = \nabla(t)$ and $\varphi_{\text{rad/cnd}} = \varphi_{\text{rad/cnd}}(t)$ develop is always the same. This is natural as they are directly proportional, $\varphi_{\text{rad/cnd}} = \frac{4c}{3} \frac{aT^4}{\kappa \rho} \nabla$. Moreover, because of Eq.(19), we see that $\varphi_{\text{rad/cnd}} < \varphi_{\text{cnd}}$ in agreement with our definition of a convective layer.

Finally, the average velocity of the convective elements remains the more sensitive variable to the physics of the star. In our case, we are limited in Fig.4, 5, and 6 to positive average velocities $\bar{v} > 0$, but the analogous analysis can be done for negative velocities $\bar{v} < 0$ with similar results. As evident from the figures, the timescale with which the asymptotic mean-stream velocity is reached by the convective elements, before dissolving by RT and KH effects, can be as short as a few hundred seconds as well as long as 10^7 seconds for bigger stars.

4.3. A numerical check

Extending the numerical investigation introduced above, allows us to propose a robust numerical study of the subsonic

regime approximations used in SFCT⁽¹⁴⁾. In particular, one of the standing hypothesis of SFCT, the limitation to subsonic regimes, translate to the condition

$$\left(\frac{\bar{v}}{\bar{R}}\right)^2 \frac{1}{2} \left(\frac{9}{4} \sin^2 \theta - 1\right) \ll A \frac{R}{\bar{R}^2} \left(\frac{3}{2} \cos \theta - \cos \phi\right) + \frac{\ddot{R}R}{\bar{R}^2}, \quad (20)$$

or

$$\left(\frac{\bar{v}\dot{R}}{\bar{R}^2}\right)^2 \frac{5}{2} \cos \theta \ll A \frac{R}{\bar{R}^2} \left(\frac{3}{2} \cos \theta - \cos \phi\right) + \frac{\ddot{R}R}{\bar{R}^2}, \quad (21)$$

that we are able now to numerically verify over an extended set of models. We proceed as follows. For the sake of simplicity we define three functions from the above Eqs.(20) and (21):

$$\begin{aligned} f(t, \theta) &\equiv \left(\frac{\bar{v}}{\bar{R}}\right)^2 \frac{1}{2} \left(\frac{9}{4} \sin^2 \theta - 1\right), \\ g(t, \theta) &\equiv \left(\frac{\bar{v}\dot{R}}{\bar{R}^2}\right)^2 \frac{5}{2} \cos \theta, \\ k(t, \theta) &\equiv A \frac{R}{\bar{R}^2} \left(\frac{3}{2} \cos \theta - \cos \phi\right) + \frac{\ddot{R}R}{\bar{R}^2}. \end{aligned} \quad (22)$$

We proceed to consider the same layer L introduced in Sec.4. Further values necessary for the computations of this exercise are available in Table 1 of P14 and the value of the derivative of \bar{v} , i.e. \dot{R} , are simply the tangents to the plot in Fig. 4, 5, or 6. We obtain for the same point inside the Sun analyzed in Sec.6.3 of P14 (after $\sim 10^6$ s) that $\bar{v} = 194.6 \text{ km s}^{-1}$, $\bar{\chi} = 8.3 \times 10^{10}$ so that at $\theta = 0$ gives $f(10^6, 0) = -6.81 \times 10^{-7}$. At the same time and location we have $\dot{v} = 1.027 \times 10^{-5} \text{ km s}^{-2}$, $\dot{\chi}' = 1.666 \times 10^5$ and $\dot{\chi}'' = 0.156$ and hence $k(10^6, 0) = 0.5$. It is evident that the first of the equations necessary to prove the Lemma 1, $f(t, \theta) \ll k(t, \theta)$, of P14 is largely verified. Now that all the values are available, it is a simple exercise to prove that also the second $g(t, \theta) \ll k(t, \theta)$.

We plot f , g , and k for any point θ or ϕ on the convective element surface in Fig.7 which makes evident that the conditions $f(t, \theta) \ll k(t, \theta)$ and $g(t, \theta) \ll k(t, \theta)$ hold in the temporal regime of interest (as mathematically proved in Lemma 1)⁽¹⁵⁾.

5. Conceptual limits and practical implications of the SFCT

5.1. On the functional timescales of the SFCT

The solution of the convective energy transport is achieved by the SFCT thanks to the uniqueness theorem (P14, Sec.6.2) which is a theorem that holds inside a *linear*-response theory framework. Hence the theory inherits the limits of this theorem, and these implications of this limitation are better understood with an example. The theorem states that, to the leading order, there is an invariant manifold solution of the system of equations

¹⁴This corresponds indeed to a numerical validation of Lemma 1 in P14

¹⁵Note how this is the contrary of what is claimed in MB16, where the authors apparently find, for the same solar model and using same equations, a failure of the conditions in Eqs.(20) and (21) that vice versa we find valid here. Motivated by this discrepancy, we have provided here all the numbers adopted in our computation *explicitly*, so that these equations can be tested easily.

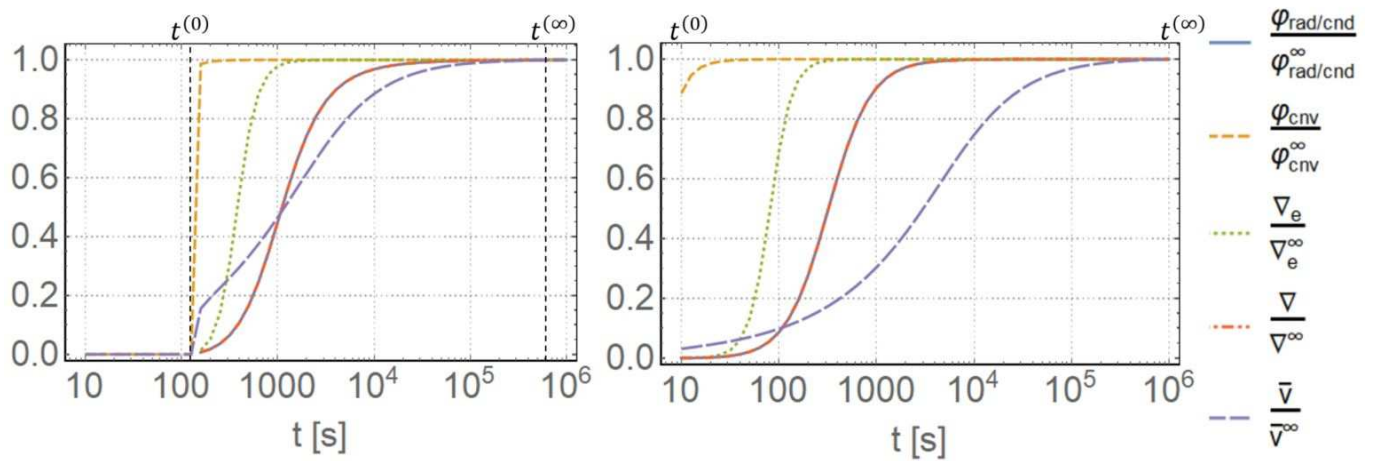


Figure 4: Evolution of the averaged fluxes, gradients and velocity for a $1M_{\odot}$ stellar model with $\log_{10}L/L_{\odot} = 0.0$, $\log_{10}T_{\text{eff}} = 3.76$ and solar metallicity. Left panel refers to $R = 0.7R_{\text{max}}$, right panel to $R = 0.88R_{\text{max}}$. We refer to $t < t^0$ as the homogeneous isotropic turbulence regime treated in Sec.3, to $t^{(0)} < t < t^{(\infty)}$ as the transition regime, and to $t < t^{(\infty)}$ as the asymptotic regime.

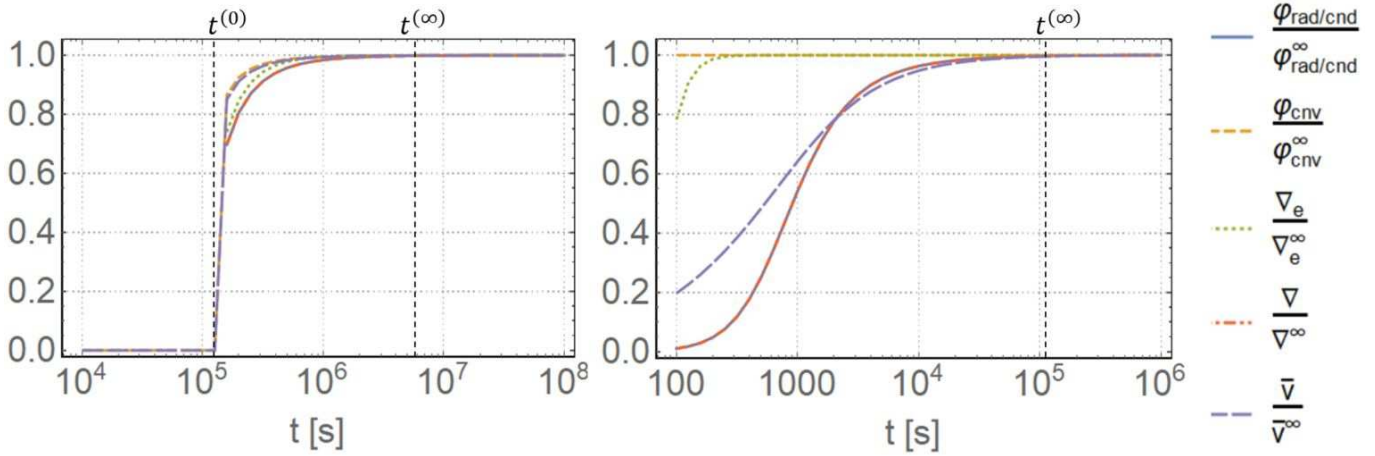


Figure 5: Same as Fig.4 but for stellar model with $\log_{10}L/L_{\odot} = 0.3$, $\log_{10}T_{\text{eff}} = 3.70$

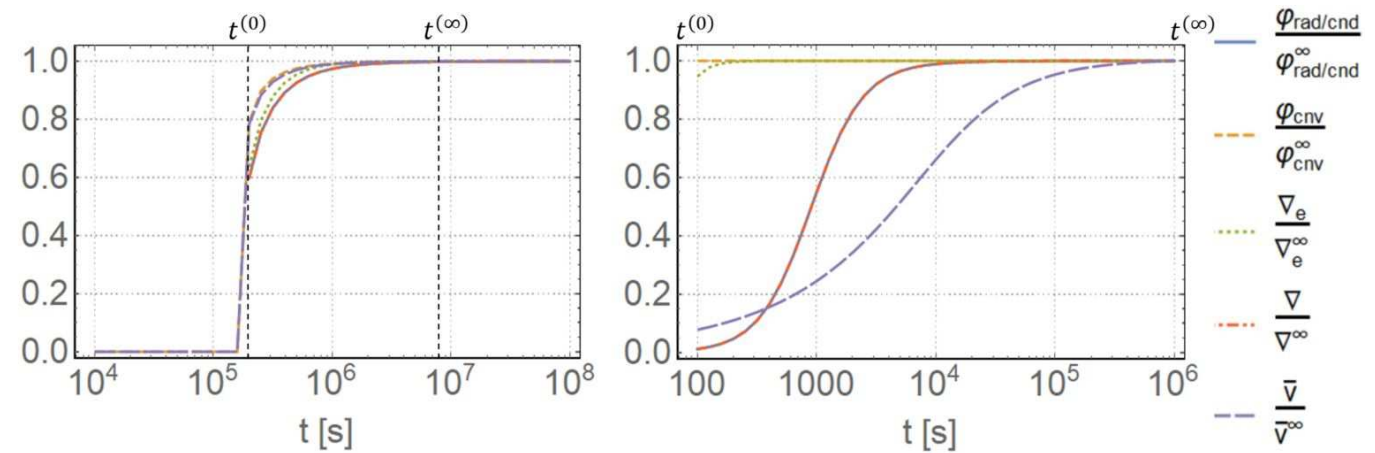


Figure 6: Same as Fig.5 but for stellar model with $\log_{10}L/L_{\odot} = 2.0$, $\log_{10}T_{\text{eff}} = 3.60$

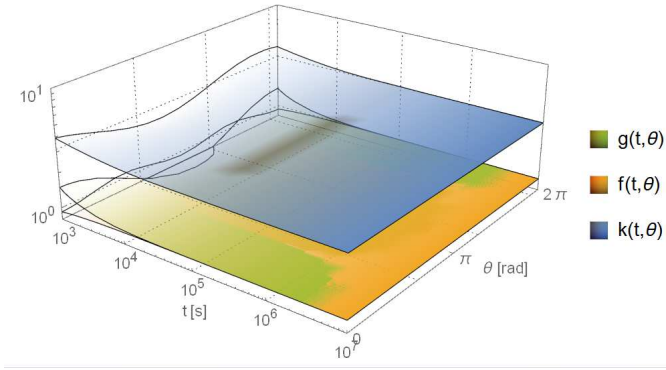


Figure 7: Numerical validation of the proof of Eq.(20) and Eq.(21). Functions are defined along the text and plotted against the values of interest, i.e. in the “asymptotic” regime of validity of the uniqueness theorem. As evident the blue manifold always overlooks the green and yellow ones for all the time-scale of interest in the development of the convection in convective unstable layers and for all the angular dependence of the equations.

of energy transfer inside a star. If an invariant solution exists, we might be tempted to get the invariance regime directly from the quintic Eq.(16) by taking to infinity the temporal limit of the coefficients Eq.(17), thus obtaining after simple manipulation:

$$\lim_{\tau \rightarrow \infty} \sum_{i=0}^5 c_i \bar{v}^i \Big|_{\chi \sim \tau^2} = \frac{1}{9} \bar{v}^2 \left(\frac{8\alpha g_4 (\nabla_{\text{ad}} - \nabla_{\text{rad}})}{\nabla_{\text{ad}}} + 9\bar{v}^3 \right) = 0.$$

Apparently, in this way we reduce the quintic to a cubic (as in the MLT case) whose only real solution for a convective region would be

$$\bar{v} = \frac{2\sqrt[3]{\alpha g_4 (\nabla_{\text{rad}} - \nabla_{\text{ad}})}}{3^{2/3} \sqrt[3]{\nabla_{\text{ad}}}}.$$

This is also confirmed by a numerical investigation of the coefficient in Eq.(17): taking $\sum_{i=0}^5 \frac{c_i \bar{v}^i}{\bar{v}^2} = 0$ and neglecting $\{c_4, c_5\} \ll \{c_1, c_2, c_3\}$ we can obtain a solution for \bar{v} in the resulting cubic that is completely indistinguishable from the \bar{v} obtained from the quintic.

Unfortunately, despite its apparent simplicity, this way of using the uniqueness theorem is wrong because it is outside its founding hypotheses. As explained in P14, the “limit $\tau \rightarrow \infty$ ” is a mathematical idealization for the dimensionless independent variable (τ in our case) to reach the asymptotic behavior of the solution, say for $t > t^\infty$. In the real situation of interest, τ cannot exceed a specific limit value securing that (i) the stellar region under consideration is still convective; (ii) the convective elements are still moving inside the convective areas; and (iii) the star itself does still exist. The state variables $p = p(\mathbf{x}; t)$, density $\rho = \rho(\mathbf{x}; t)$, and temperature $T = T(\mathbf{x}; t)$, set the real physical limit “ $\tau \rightarrow \infty$ ” (or “ $\tau \rightarrow \partial L$ ” in the example of Sec.3, τ normalized time), so that the limit of Eq.(18):

$$\lim_{\tau \rightarrow \infty} \alpha = \lim_{\tau \rightarrow \infty} \frac{acT^3}{\kappa\rho^2c_p},$$

is coherently accounted for. However, the star at an infinite time does not exist any longer, and it is simple to prove that

the modelling scheme for the SFCT flattens the state variable gradients to adiabatic stratifications: $\lim_{\tau \rightarrow \infty} \nabla = \lim_{\tau \rightarrow \infty} \nabla_e = \nabla_{\text{ad}}$ and the size of the convective element would diverge $\lim_{\tau \rightarrow \infty} \chi = \infty$ as expected (note indeed that one of the primary effects of the convection is to homogenize a stellar gradient).

To conclude, there is non mathematical shortcut to the quintic in Eq.(16) because of its physical implications.

5.2. On the effect of the turbulence

One of the known present limitations of the SFCT is the missing treatment of the turbulence. We know that turbulence is one of the critical physical phenomena to consider, and we assume it to affect the SFCT both in the onset of the convection, e.g., in Fig.4, 5, and 6 for $t < t^{(0)}$, and at its asymptotic regime, say for $t > t^{(\infty)}$ in Fig.4, 5, and 6. Nevertheless, for problems of interest to us as the generation of stellar tracks, the turbulence is well known to be irrelevant: results as from, e.g., Brown et al. (2005), clearly show how stellar tracks based on turbulence-free theory such as the MLT are well capable of reproducing stellar isochrones that fit globular cluster stars from the main sequence up to the red-giant branch. MLT does not include any correction due to turbulence. Results as the ones shown in Brown et al. (2005) can indeed well be claimed as some of the most reliable proof of the validity of the MLT framework, and in turn, on the second-order relevance of the turbulent convection in reproducing true stellar observations.

Here, we can try to understand the role of the exchange of energy between the mean convective flow and the turbulence in the regime $t > t^{(\infty)}$. The regime $t < t^{(0)}$, introduced in Sec.3.1 as a limiting case for the SFCT in a homogeneous isotropic medium, is hence not of interest.

If we assume that the turbulent cascade distribution function of the stellar plasma in S_0 is given by $f_0 = f_0(\mathbf{x}, \mathbf{v}; t)$ then, the mean convective flow is just the first order moment of this distribution $\bar{\mathbf{v}}_0 = \int \mathbf{v}_0 f_0(\mathbf{x}, \mathbf{v}; t) d^3\mathbf{x}$, while the second-order centered moment is $\sigma_0^2 = \int (\mathbf{v}_0 - \bar{\mathbf{v}}_0)^{\otimes 2} f_0 d^3\mathbf{x}$ (with $^{\otimes n}$ the ordinary tensor product of order n). Because we are interested only in the case of the asymptotic regime $t > t^{(\infty)}$, we simplify the previous as $\int \mathbf{v}_0 f_0(\mathbf{x}, \mathbf{v}; t > t^{(\infty)}) d^3\mathbf{x} = \mathbf{v}_0^\infty$ and similarly for σ_0^∞ (we omit the square which is present here only for a historical reason while clearly σ can have negative cross terms.) It is simple to prove that the relation between the first and second moments is $\sigma_0^2 = \overline{\mathbf{v}_0^{\otimes 2}} - \bar{\mathbf{v}}_0 \bar{\mathbf{v}}_0$. If we time-average the Navier-Stokes equations (then usually referred as Reynolds-averaged Navier-Stokes), i.e., we get:

$$\langle \mathbf{v}_0^\infty, \nabla_x \rangle \mathbf{v}_0^\infty + \overline{\langle \mathbf{v}_0 - \mathbf{v}_0^\infty, \nabla_x \rangle (\mathbf{v}_0 - \mathbf{v}_0^\infty)} = \nabla_x \frac{p^\infty}{\rho^\infty} \quad (23)$$

Moreover, noticing that the contribution from $\langle \langle \mathbf{v}_0^\infty, \nabla_x \rangle, \mathbf{v}_0 - \mathbf{v}_0^\infty \rangle$ and $\langle \mathbf{v}_0 - \mathbf{v}_0^\infty, \nabla_x \rangle \mathbf{v}_0^\infty$ cancel out when time-averaged, we arrive at the version of the Reynolds-averaged Navier-Stokes suited to our purpose:

$$\begin{aligned} \langle \mathbf{v}_0^\infty, \nabla_x \rangle \mathbf{v}_0^\infty &= -\nabla_x \frac{p^\infty}{\rho^\infty} + \overline{\langle \nabla_x, -(\mathbf{v}_0 - \mathbf{v}_0^\infty) (\mathbf{v}_0 - \mathbf{v}_0^\infty) \rangle} \\ &= -\nabla_x \frac{p^\infty}{\rho^\infty} - \langle \nabla_x, \sigma_0 \rangle. \end{aligned} \quad (24)$$

While this equation holds within any small layer L , $p^\infty = \text{cst.}$ and $\rho^\infty = \text{cst.}$, pressure and density retain their spatial dependence within the convective zone V supposedly composed of several layers. At different L , and within V , we have that $p^\infty = p^\infty(\mathbf{x})$ and $\rho = \rho^\infty(\mathbf{x})$. Because of the results in Fig.4, 5, and 6 the temporal dependence can be safely omitted as the structure of the star is unchanged over the time interval $\Delta t \simeq t^\infty$ of interest here. Eq.(24) couples the mean flow \mathbf{v}^∞ , to the dispersion velocity σ_0^∞ , i.e., to the statistical index of the turbulent motions of the stellar plasma. The components of $\boldsymbol{\tau} \equiv \rho\sigma_0$ are indeed traditionally called the “Reynolds stresses” and have been the subject of extensive study related to the problem of the closure of the moment equations of f_0 (e.g., Pope, 2000; Launder and Sandham, 2002).

For $t > t^\infty$, the i^{th} component of the force acting on a surface element due to σ_0^∞ is written, e.g., as $\rho^\infty \sigma_0^\infty d^2S$, so that for $t > t^\infty$ the rate of work \dot{W}^∞ due to turbulent motions follows as $\rho^\infty \langle \mathbf{v}_0^\infty, \sigma_0^\infty d^2S \rangle$ for the whole convective shell of volume V bounded by the surface S and we can write:

$$\frac{d}{dt}W^\infty = \oint_S \langle \mathbf{v}_0^\infty, \rho^\infty \sigma_0^\infty d^2S \rangle = \int_V \rho^\infty \langle \nabla_x, \mathbf{v}_0^\infty \sigma_0^\infty \rangle d^3V, \quad (25)$$

where on the last equality we used Gauss’s theorem. Hence, for a unit volume, we have that

$$\begin{aligned} \frac{d}{d^3V} \frac{d}{dt}W^\infty &= \langle \nabla_x, \mathbf{v}_0^\infty \sigma_0^\infty \rangle \\ &= \rho^\infty \langle \nabla_x, \sigma_0^\infty \rangle \mathbf{v}_0^\infty + \rho^\infty \sigma_0^\infty \langle \nabla_x, \mathbf{v}_0^\infty \rangle, \end{aligned} \quad (26)$$

thus identifying the meaning of $\rho^\infty \langle \nabla_x, \sigma_0^\infty \rangle$ also as a force. Because we defined σ_0^∞ just from an average procedure on the (unknown) distribution function, σ_0^∞ cannot create or destroy mechanical energy. Instead, σ_0^∞ can only represent the rate of change of kinetic energy per unit of volume. For simplicity of argument, we exclude over/under-shooting of the convective elements so that we can safely assume we can null the convective flux at the boundary of the convective zone V , thus that the divergence $\langle \nabla_x, \mathbf{v}_0^\infty \sigma_0^\infty \rangle$ statistically cancels out and the previous Eq.(26) balances the LHS with the RHS as follows:

$$\int -\rho^\infty \langle \nabla_x, \sigma_0^\infty \rangle \mathbf{v}_0^\infty dV = \int \sigma_0^\infty \rho^\infty \langle \nabla_x, \mathbf{v}_0^\infty \rangle dV. \quad (27)$$

Hence, if $\rho^\infty \langle \nabla_x, \sigma_0^\infty \rangle$ is the force due to σ_0^∞ (per unit volume acting) on the mean flow, then $\rho^\infty \langle \nabla_x, \sigma_0^\infty \rangle \mathbf{v}_0^\infty$ is the rate of work of this force, and $-\rho^\infty \langle \nabla_x, \sigma_0^\infty \rangle \mathbf{v}_0^\infty$ the rate of loss of kinetic energy from the mean flow as a result of the turbulence that must equal precisely the rate of gain of the kinetic energy by the turbulence. Under the light of these considerations, it is evident from Eq.(27), that σ_0^∞ gives rise to a net force acting on the mean flow whose rate of work is negative meaning that the mean flow loses energy to the turbulence, i.e., energy is transferred from the mean flow to the turbulence.

Concluding, we have proved that the mean flow is overestimated by the SFCT that, at the present stage, can provide only

an upper limit to the convective flux (even if in a better way than what MLT does because it is a parameter-free theory).

It remains beyond the goal of the present paper to upgrade the SFCT to account for the turbulence cascade. In the light of the results in P16, it is probably not necessary for stellar tracks. Several approaches are available in the literature to account for turbulence parametrically, as well as the results of hydrodynamics 3D simulations (e.g., Arnett et al., 2015) to which we refer the interested reader. See also Kupka and Muthsam (2017) for a recent review.

6. Conclusions

In this work, we investigated in some detail the key elements of the SFCT, in particular the pressure treatment. We have:

- presented the pressure treatment of the SFCT in the limiting case of homogeneous isotropic intrastellar plasma and compared it with the MLT;
- presented a numerical validation of the SFCT equations with the simplest solar model available in the literature that complements the analytical treatment of P14;
- obtained the first numerical temporal estimations of the onset of the convection in a convective layer thus evidencing for the first time (numerically) a temporal dependence of classical Schwarzschild or Ledoux criteria that was not previously studied;
- remarked on the limitation of the SFCT regarding temporal integration and the treatment of turbulence.

Finally, in light of the above considerations, it is instructive to consider why the MLT captures to a good approximation the essence of the transport of energy inside a star. This happens because MLT contains a free parameter whose meaning is not to merely quantify the distance travelled by “an average” eddy along the vertical direction inside a star, but also to take somehow into account the whole phenomenon of the turbulence cascade of energy, the transmission of the energy to the flux, the interaction between eddies, and the complex pressure information transmission from a place to another, etc.

The MLT is not a hydrodynamic theory because no time evolution is considered in it. Therefore the question how far a convective element can travel has no simple physical meaning because there is no such a simple connection between the average motion of the turbulent eddies and the pressure scale length: the pressure scale length is a natural scale length of a star that is related to the dynamics of the convective elements through Eq.(1) whereas the mixing-length, in reality, has little to do, if nothing at all, with a length or a radial motion. As a matter of fact the most successful models of turbulence do not actually deal with spherical bodies but rather with tube-like objects, even though the classic “view” of turbulence relates the transport of energy from large to small scales with a mechanism that passes from convective elements as blobs, to rolled up vortex sheets in a sequence of azimuthal vorticity, and to poloidal motions that

sweep angular momentum outward radially to form sheets (e.g., Kuo and Corrsin, 1972).

The simple exercises we have described here cannot adequately capture the whole physical complexity of magnetic and turbulent convection at work in the real star. This is in part captured by the study of P14. Nevertheless, the discussion presented here is valuable in clarifying the role played by the essential ingredients of the stellar convection, at least to the order required to reproduce the observed HR-diagrams.

The success of the SFCT is evident in the quality of the stellar models it generates (see P16) which nicely fit the positions of stars in the Hertzsprung-Russell $\{\lg T_{eff}, \lg L/L_{\odot}\}$ diagrams by continuously adapting itself to the ever-changing properties of a star during its evolutionary history and without requiring an external calibration on standard stars like the Sun. Moreover, the mathematical exploitation of the uniqueness theorem in P14 can open new possibilities not only to eliminate of parameters whose nature and physical meaning are far from being clear (e.g., the mixing-length) but also to investigate closure relations of the hierarchy of hydrodynamic equations (e.g., Launder and Sandham, 2002).

The internal structure of stars can also be probed with other techniques such as deep helio-seismology and giro-seismology studies. Nevertheless, the SFCT constitutes a step forward with respect to the classical MLT with which it shares the significant merits of simplicity and easy usage, but which surpasses by eliminating the so-called mixing length parameter. The SFCT does not intend to replace or compete with more sophisticated theories of convection and 3D numerical simulations that, however, appear to be still far from being readily incorporable into large stellar model datasets.

Acknowledgements

We thank J. Kollmeier and E. K. Grebel for a careful reading of an early version of this manuscript and for many constructive suggestions. This work benefited from support by the National Science Foundation under Grant No. PHY-1430152 (JINA Centre for the Evolution of the Elements) and NASA grant No. NNX14AF84G.

Arnett, W. D., Meakin, C., Viallet, M., Campbell, S. W., Lattanzio, J. C., Mocák, M., Aug. 2015. Beyond Mixing-length Theory: A Step Toward 321D. *ApJ* 809, 30.
 Batchelor, G. K., Feb. 2000. An Introduction to Fluid Dynamics.
 Batchelor, G. K., Proudman, I., Jan. 1956. The Large-Scale Structure of Homogeneous Turbulence. *Philosophical Transactions of the Royal Society of London Series A* 248, 369–405.
 Bec, J., Biferale, L., Cencini, M., Lanotte, A. S., Toschi, F., Mar. 2010. Intermittency in the velocity distribution of heavy particles in turbulence. *Journal of Fluid Mechanics* 646, 527.
 Benzi, R., Biferale, L., Fisher, R., Lamb, D. Q., Toschi, F., Jun. 2010. Inertial range Eulerian and Lagrangian statistics from numerical simulations of isotropic turbulence. *Journal of Fluid Mechanics* 653, 221–244.
 Bernard, P. S., Aug. 1983. Kinematics of velocity and vorticity correlations in turbulent flow. *Physics of Fluids* 26, 2080–2087.
 Bertelli, G., Girardi, L., Marigo, P., Nasi, E., Jun. 2008. Scaled solar tracks and isochrones in a large region of the Z-Y plane. I. From the ZAMS to the TP-AGB end for 0.15-2.5 M_{\odot} stars. *A&A* 484, 815–830.
 Biermann, L., 1951. Bemerkungen über das Rotationsgesetz in irdischen und stellaren Instabilitätszonen. Mit 1 Textabbildung. *ZAp* 28, 304.

Böhm-Vitense, E., 1958. Über die Wasserstoffkonvektionszone in Sternen verschiedener Effektivtemperaturen und Leuchtkräfte. Mit 5 Textabbildungen. *ZAp* 46, 108.
 Brown, T. M., Ferguson, H. C., Smith, E., Guhathakurta, P., Kimble, R. A., Sweigart, A. V., Renzini, A., Rich, R. M., VandenBerg, D. A., Oct. 2005. Stellar Cluster Fiducial Sequences with the Advanced Camera for Surveys. *AJ* 130, 1693–1706.
 Chiosi, C., Chiosi, E., Pasetto, S., 2017. submitted. submitted to MNRAS .
 Couch, S. M., Chatzopoulos, E., Arnett, W. D., Timmes, F. X., Jul. 2015. The Three-dimensional Evolution to Core Collapse of a Massive Star. *eapj@ApJLetters* 808, L21.
 Cox, J. P., Giuli, R. T., 1968. Principles of stellar structure - Vol.1: Physical principles; Vol.2: Applications to stars.
 Cristini, A., Meakin, C., Hirschi, R., Arnett, D., Georgy, C., Viallet, M., Walkington, I., Oct. 2017. 3D hydrodynamic simulations of carbon burning in massive stars. *MNRAS* 471, 279–300.
 da Silva, C. B., Hunt, J. C. R., Eames, I., Westerweel, J., Jan. 2014. Interfacial Layers Between Regions of Different Turbulence Intensity. *Annual Review of Fluid Mechanics* 46, 567–590.
 Davidson, P. A., Nov. 2010. On the decay of Saffman turbulence subject to rotation, stratification or an imposed magnetic field. *Journal of Fluid Mechanics* 663, 268–292.
 Davidson, P. A., Okamoto, N., Kaneda, Y., Sep. 2012. On freely decaying, anisotropic, axisymmetric Saffman turbulence. *Journal of Fluid Mechanics* 706, 150–172.
 Forster, D., Nelson, D. R., Stephen, M. J., Aug. 1977. Large-distance and long-time properties of a randomly stirred fluid. *Phys. Rev. A* 16, 732–749.
 Frisch, U., 1998. Turbulence: The Legacy of A. N. Kolmogorov. *Astrophysical Letters and Communications* 35, 463.
 Gastine, T., Wicht, J., Aurnou, J. M., Sep. 2015. Turbulent Rayleigh-Bénard convection in spherical shells. *Journal of Fluid Mechanics* 778, 721–764.
 George, W. K., Jul. 1992. The decay of homogeneous isotropic turbulence. *Physics of Fluids A* 4, 1492–1509.
 Glatzmaier, G. A., 2013. Introduction to Modelling Convection in Planets and Stars.
 Goode, S., Annin, S., 2015. Differential Equations and Linear Algebra.
 Hanazaki, H., Hunt, J. C. R., 1996. Linear processes in unsteady stably stratified turbulence. *Journal of Fluid Mechanics* 318, 303–337.
 Hotta, H., Rempel, M., Yokoyama, T., Jan. 2015. High-resolution Calculation of the Solar Global Convection with the Reduced Speed of Sound Technique. II. Near Surface Shear Layer with the Rotation. *ApJ* 798, 51.
 Hunt, J. C. R., Carruthers, D. J., Mar. 1990. Rapid distortion theory and the 'problems' of turbulence. *Journal of Fluid Mechanics* 212, 497–532.
 Ishihara, T., Gotoh, T., Kaneda, Y., Jan. 2009. Study of High - Reynolds Number Isotropic Turbulence by Direct Numerical Simulation. *Annual Review of Fluid Mechanics* 41, 165–180.
 Jackson, J. D., 1975. Classical electrodynamics.
 Jiang, Y.-F., Cantiello, M., Bildsten, L., Quataert, E., Blaes, O., Nov. 2015. Local Radiation Hydrodynamic Simulations of Massive Star Envelopes at the Iron Opacity Peak. *ApJ* 813, 74.
 Kellogg, O. K., Mar. 1929. Foundations of potential theory.
 Kippenhahn, R., Weigert, A., 1994. Stellar Structure and Evolution.
 Kippenhahn, R., Weigert, A., Weiss, A., 2012. Stellar Structure and Evolution.
 Kitamura, T., Nagata, K., Sakai, Y., Sasoh, A., Terashima, O., Saito, H., Harasaki, T., Jan. 2014. On invariants in grid turbulence at moderate Reynolds numbers. *Journal of Fluid Mechanics* 738, 378–406.
 Kitiashvili, I. N., Kosovichev, A. G., Mansour, N. N., Wray, A. A., Apr. 2016. Dynamics of Turbulent Convection and Convective Overshoot in a Moderate-mass Star. *eapj@ApJLetters* 821, L17.
 Kolmogorov, A., 1941. The Local Structure of Turbulence in Incompressible Viscous Fluid for Very Large Reynolds' Numbers. *Akademiia Nauk SSSR Doklady* 30, 301–305.
 Kuo, A. Y.-S., Corrsin, S., 1972. Experiment on the geometry of the fine-structure regions in fully turbulent fluid. *Journal of Fluid Mechanics* 56, 447–479.
 Kupka, F., Muthsam, H. J., Jul 2017. Modelling of stellar convection. *Living Reviews in Computational Astrophysics* 3 (1), 1.
 Kuznetsov, E., Newell, A. C., Zakharov, V. E., Dec. 1991. Intermittency and turbulence. *Physical Review Letters* 67, 3243–3246.
 Landau, L. D., Lifshitz, E. M., 1959. Fluid mechanics.
 Launder, B. E., Sandham, N. D., Mar. 2002. Closure Strategies for Turbulent

- and Transitional Flows.
- Layek, G. C., Sunita, Oct. 2017. On the nature of multitude scalings in decaying isotropic turbulence. *International Journal of Non Linear Mechanics* 95, 143–150.
- Lebedev, N. N., Silverman, R. A., Livhtenberg, D. B., 1965. *Special Functions and Their Applications*. *Physics Today* 18, 70.
- Lecoanet, D., Schwab, J., Quataert, E., Bildsten, L., Timmes, F. X., Burns, K. J., Vasil, G. M., Oishi, J. S., Brown, B. P., Nov. 2016. Turbulent Chemical Diffusion in Convectively Bounded Carbon Flames. *ApJ* 832, 71.
- Lee, D. A., Tan, H. S., Jun. 1967. Study of Inhomogeneous Turbulence. *Physics of Fluids* 10, 1224–1230.
- Lohse, D., Xia, K.-Q., Jan. 2010. Small-Scale Properties of Turbulent Rayleigh-Bénard Convection. *Annual Review of Fluid Mechanics* 42, 335–364.
- Meldi, M., Sagaut, P., Lucor, D., Feb. 2011. A stochastic view of isotropic turbulence decay. *Journal of Fluid Mechanics* 668, 351–362.
- Meneveau, C., Jan. 2011. Lagrangian Dynamics and Models of the Velocity Gradient Tensor in Turbulent Flows. *Annual Review of Fluid Mechanics* 43, 219–245.
- Miller Bertolami, M. M., Viallet, M., Prat, V., Barsukow, W., Weiss, A., Apr. 2016. On the relevance of bubbles and potential flows for stellar convection. *MNRAS* 457, 4441–4453.
- Moffatt, H. K., May 1981. Some developments in the theory of turbulence. *Journal of Fluid Mechanics* 106, 27–47.
- Moffatt, H. K., 2002. G.k. batchelor and the homogenization of turbulence. *Annual Review of Fluid Mechanics* 34, 19–35.
- Ossia, S., Lesieur, M., Dec. 2000. Energy backscatter in large-eddy simulations of three-dimensional incompressible isotropic turbulence. *Journal of Turbulence* 1, 010.
- Pasetto, S., Bertelli, G., Grebel, E. K., Chiosi, C., Fujita, Y., Jun. 2012. Dissipative phenomena in extended-body interactions. I. Methods: Dwarf galaxies of the Local Group and their synthetic CMDs. *A&A* 542, A17.
- Pasetto, S., Chiosi, C., Chiosi, E., Cropper, M., Weiss, A., Jul. 2016. Theory of stellar convection - II. First stellar models. *MNRAS* 459, 3182–3202.
- Pasetto, S., Chiosi, C., Cropper, M., Grebel, E. K., Dec. 2014. Theory of stellar convection: removing the mixing-length parameter. *MNRAS* 445, 3592–3609.
- Pasetto, S., Cropper, M., Fujita, Y., Chiosi, C., Grebel, E. K., Jan. 2015. Environmental effects on star formation in dwarf galaxies and star clusters. *A&A* 573, A48.
- Plesset, M. S., Jan. 1954. On the Stability of Fluid Flows with Spherical Symmetry. *Journal of Applied Physics* 25, 96–98.
- Pope, S. B., Aug. 2000. *Turbulent Flows*.
- Poujade, O., Peybernes, M., Jan. 2010. Growth rate of Rayleigh-Taylor turbulent mixing layers with the foliation approach. *Phys. Rev. E* 81 (1), 016316.
- Prandtl, L., 1925. Bericht Äijber Untersuchungen zur ausgebildeten Turbulenz. *Math. Meth.* 5, 136–139.
- Press, W. H., Teukolsky, S. A., Vetterling, W. T., Flannery, B. P., 1992. *Numerical recipes in FORTRAN. The art of scientific computing*.
- Rempel, M., Cheung, M. C. M., Apr. 2014. Numerical Simulations of Active Region Scale Flux Emergence: From Spot Formation to Decay. *ApJ* 785, 90.
- Rieutord, M., Rincon, F., Jun. 2010. The Sun’s Supergranulation. *Living Reviews in Solar Physics* 7, 2.
- Rincon, F., Roudier, T., Schekochihin, A. A., Rieutord, M., Mar. 2017. Supergranulation and multiscale flows in the solar photosphere. Global observations vs. a theory of anisotropic turbulent convection. *A&A* 599, A69.
- Rose, W. G., 1966. Results of an attempt to generate a homogeneous turbulent shear flow. *Journal of Fluid Mechanics* 25, 97–120.
- Saffman, P. G., 1967. The large-scale structure of homogeneous turbulence. *Journal of Fluid Mechanics* 27, 581–593.
- Sagaut, P., 2008. BOOK REVIEW: *Homogeneous Turbulence Dynamics*.
- Schmidt, W., Federrath, C., Apr. 2011. A fluid-dynamical subgrid scale model for highly compressible astrophysical turbulence. *A&A* 528, A106.
- Schumacher, J., Scheel, J. D., Krasnov, D., Donzis, D. A., Yakhot, V., Sreenivasan, K. R., Jul. 2014. Small-scale universality in fluid turbulence. *Proceedings of the National Academy of Science* 111, 10961–10965.
- Skrbek, L., Stalp, S. R., Aug. 2000. On the decay of homogeneous isotropic turbulence. *Physics of Fluids* 12, 1997–2019.
- Soulard, O., Griffond, J., Gréa, B.-J., Sep. 2015. Large-scale analysis of unconfined self-similar Rayleigh-Taylor turbulence. *Physics of Fluids* 27 (9), 095103.
- Teitelbaum, T., Mininni, P. D., Dec. 2012. Decay of Batchelor and Saffman rotating turbulence. *Phys. Rev. E* 86 (6), 066320.
- Weiss, A., Hillebrandt, W., Thomas, H.-C., Ritter, H., 2004. *Cox and Giuli’s Principles of Stellar Structure*.
- Yakhot, V., Oct. 2014. Reynolds number of transition and self-organized criticality of strong turbulence. *Phys. Rev. E* 90 (4), 043019.
- Zhou, Y., Dec. 2017. Rayleigh-Taylor and Richtmyer-Meshkov instability induced flow, turbulence, and mixing. I. *Phys. Rep.* 720, 1–136.

Appendix A. Non-inertial linear response theory for convective elements in spherical coordinates

We summarize here some results of the non-inertial response theory for non-degenerate non-relativistic gas instabilities in spherical coordinates developed by Pasetto et al. (2015). This theory provides the context from which the SFCT is derived as a particular case. Our summary here is meant to clarify and better explain some of the assumptions made by P14 and also to highlight some of the considerations made in the present paper, in particular those about the fate of convective elements.

We limit ourselves to consider the convective elements as blobs of constant density ρ_e , slightly different from that of the stellar medium, with density ρ , at any generic location \mathbf{r} inside a spherical star centered in the inertial reference frame S_0 . The ideal surface (spherical) enclosing and separating the convective element from the rest of the medium is indicated with $\mathbb{S}^2 : \Sigma(\xi, \theta, \phi; t)$ and is implicitly defined by an equation of the type:

$$\Sigma(\xi, \theta, \phi; t) \equiv \xi - (\xi_e(t) + \eta(t) Y_l^m(\theta, \phi)), \quad (\text{A.1})$$

where Y_l^m are the spherical harmonics (e.g., Lebedev et al., 1965) for $\theta \in [0, \pi[$, $\phi \in [0, 2\pi[$ and $\eta(t) \ll \xi_e(t) \forall t$ is the radial perturbation of the unperturbed radius $\xi = \xi_e$ of the convective element. For this summary presentation, we will make use of the non-spherical perturbation of Eq.(A.1) and highlight the various topics under examination, however without proving the results which can be instead found in Appendix A of Pasetto et al. (2015).

Because a generic convective element forms from a density perturbation of the surrounding pre-existing stellar medium, there is undoubtedly continuity between the medium inside and outside the convective element at the surface Σ , i.e., the stellar medium satisfies the continuity equations on both sides of the surface Σ :

$$\begin{cases} \frac{\partial \Sigma}{\partial t} + \langle \nabla_{\xi} \varphi_{e,v_1}, \nabla_{\xi} \Sigma \rangle = 0 \\ \frac{\partial \Sigma}{\partial t} + \langle \nabla_{\xi} \varphi_{v_1}, \nabla_{\xi} \Sigma \rangle = 0, \end{cases} \quad (\text{A.2})$$

where these conditions on the potential-flows φ_{e,v_1} inside the convective element, and in the stellar medium φ_{v_1} are approximated to the leading order by:

$$\begin{aligned} \varphi_{e,v_1} &\cong \xi^l Y_l^m \left(\frac{\dot{\eta}}{l} \xi_e^{l-1} + \frac{2\eta}{l} \dot{\xi}_e \xi_e^{l-1} \right) - \frac{\xi_e^2 \dot{\xi}_e}{\xi}, \\ \varphi_{v_1} &\cong -v \cos(\theta) \xi \left(1 + \frac{1}{2} \frac{\xi_e^3}{\xi^3} \right) - \frac{\xi_e^2 \dot{\xi}_e}{\xi} - \frac{3\xi_e^{l+1}}{(l+1)\xi^{l+1}} \\ &\quad \eta \left(\frac{v}{2} \frac{\partial Y_l^m}{\partial \theta} \sin \theta + Y_l^m \left(\frac{1}{3} \frac{\dot{\eta}}{\eta} \xi_e + \frac{2}{3} \frac{\dot{\xi}_e}{\xi_e} + v \cos \theta \right) \right), \end{aligned} \quad (\text{A.3})$$

respectively (see Appendix A Pasetto et al., 2015). A convective element carries in its interior the stellar plasma which is at rest in S_1 , i.e., no external flow is allowed to deeply penetrate inside the convective element (at the first order) as long as the convective element retains its identity. Therefore, the difference between the two equations (A.3) is limited to the velocity term present in the second equation and missing in the first one. It is easy to prove that for $\eta \rightarrow 0$ we recover the familiar potential flow approximation which is the basis of different studies, e.g., the pressure exerted by the intergalactic medium on dwarf galaxies (see Eq.(6) in Pasetto et al., 2012), the dynamics of the potential flow approximation for stellar convection in P14, etc.

At the surface radius $\|\xi\| = \xi_e + \eta Y_l^m$ we impose the condition of continuity for the stress vectors \mathbf{s} in the inviscid approximation: $\langle \hat{\mathbf{n}}, \mathbf{s} \rangle_{\Sigma=0} = \langle \hat{\mathbf{n}}, \mathbf{s}_e \rangle_{\Sigma=0}$. This can be calculated with the aid of Eq.(A.3) and two energy conservation equations for the stellar medium (see Eq.(7) of Pasetto et al., 2012):

$$\frac{\partial \varphi_{v_1}}{\partial t} + \frac{1}{2} \langle \nabla_{\xi} \varphi_{v_1}, \nabla_{\xi} \varphi_{v_1} \rangle + \frac{P}{\rho} = f(t) - \langle \mathbf{a}_O, \xi \rangle \quad (\text{A.4})$$

and its analogues for φ_{e,v_1} . The time dependent function f is fixed by assuming hydrostatic equilibrium far away from Σ .

In P14 the treatment of the stellar convection is simplified by assuming (i) subsonic regime, (ii) hydrostatic equilibrium for the star and (iii) neglecting fluid treatment inside the convective element which is allowed merely to radiate from Σ . While the first two hypotheses have been extensively commented on previous studies (P14, Pasetto et al., 2015, and here), the third one can be easily understood as follows. A convective element density is only slightly different from that of the surrounding medium so that dissipative processes will act rapidly during its expansion. This implies that in such a case we can neglect self-gravity and ignore the Poisson equation for the matter contained in its interior. The loss of energy by the convective elements Eq.(60) of P14 is supposed to be only due to radiation from the surface where the radiative transfer equation is accounted. No mechanical dissolution of the convective elements is considered thus they keep their spherical shape until the end of their life. This approximation (apparently too

restrictive for the purposes of Pasetto et al. (2015)) turned out to be acceptable if one looks at the overall structure of stellar models calculated with the SFCT plus suitable boundary conditions (e.g., Pasetto et al., 2016; Chiosi et al., 2017).

Furthermore, by retaining the third hypotheses, we can rapidly derive an instability criterion that allows an understanding of the survival of the convective elements as they expand/contract moving upward/downward in an unstable convective layer as already mentioned in Section 3.3. By developing the algebra in full (see Eq.A30 in Pasetto et al., 2015, for more details) we reach the criterion expressed by the quantity $\gamma^2 > 0$ (defined below) which allows us to investigate the onset of instabilities and the resulting dissolution of convective elements¹⁶. The quantity γ^2 is defined as follows (RT and KH stand for Rayleigh-Taylor and Kelvin-Helmholtz respectively as introduced above):

$$\gamma^2 = \gamma_{\text{RT}}^2 + \gamma_{\text{a-RT}}^2 + \gamma_{\text{mix}}^2 + \gamma_{\text{KH}}^2 + \gamma_I^2 \quad (\text{A.5})$$

$$\left\{ \begin{array}{l} \gamma_{\text{RT}}^2 \equiv \frac{3A_+ (3A_+ v^{\parallel} + 8\xi_e)}{(4\xi_e)^2} v^{\parallel} \\ \gamma_{\text{a-RT}}^2 \equiv \frac{a_{\text{O}}^{\parallel} (4lA - A_+)}{2 \cdot 2\xi_e} \\ \gamma_{\text{mix}}^2 \equiv \frac{9 \cdot 2A_{--} A_+ F_1}{4 (2\xi_e)^2} v^{\parallel} v^{\perp} \\ \gamma_{\text{KH}}^2 \equiv \frac{9 v^{\perp 2} (A - 2(l_- + F_2) + F_1^2) + A}{4 (2\xi_e)^2} \\ \gamma_I^2 \equiv \frac{1}{2} \left(\frac{3\xi_e^2}{2\xi_e^2} + \frac{A(1+2l)\xi_e}{\xi_e} \right), \end{array} \right.$$

where the quantity A is the generalized Atwood's number

$$A \equiv \frac{l_+ l_{++} \rho_e - l_- l \rho}{l_+ \rho_e + l \rho},$$

and F_1 and F_2 are two special function defined in Appendix B of Pasetto et al. (2015):

$$F_1 \equiv \frac{1}{Y_l^m} \frac{\partial Y_l^m}{\partial \theta} \quad \text{and} \quad F_2 \equiv \frac{1}{Y_l^m} \frac{\partial^2 Y_l^m}{\partial \theta^2}.$$

The other quantities are $l_+ \equiv l + 1$, $l_{++} \equiv l + 2$, $A_- \equiv A - 1$, $A_{--} \equiv A - 2$, etc. and $v^{\parallel} \equiv v \cos \theta$ \wedge $v^{\perp} \equiv v \sin \theta$. The nature and the role of the single terms in Eq.(A.5) are reviewed in Section 3.3 and Pasetto et al. (2015) where an extended analysis is made, and peculiar limits are treated. Here we limit ourselves to remark on the asymmetric role that RT and KH instabilities have in the building up of γ^2 in that while to the leading order the RT instability retains a dependence on the acceleration and velocity, i.e., both γ_{RT}^2 and $\gamma_{\text{a-RT}}^2$ survive the linearization of the equations, the KH instability contribution γ_{KH}^2 , depends only on the velocity because its dependence on the acceleration is of the order of $O(\eta^2)$.

¹⁶Traditionally the instability is indicated as γ^2 and not as γ . Although it can happen that $\gamma^2 < 0$, the γ^2 is kept only for historical reasons and to save the connection with older studies.